






Article

A New Fractional-Order Chaotic System with Its Analysis, Synchronization, and Circuit Realization for Secure Communication Applications

Zain-Aldeen S. A. Rahman ^{1,2}, Basil H. Jasim ², Yasir I. A. Al-Yasir ^{3,*}, Yim-Fun Hu ³, Raed A. Abd-Alhameed ³ and Bilal Naji Alhasnawi ²

¹ Department of Electrical Techniques, Technical Institute/Qurna, Southern Technical University, Basra 61016, Iraq; as.zain9391@stu.edu.iq

² Department of Electrical Engineering, College of Engineering, University of Basrah, Basra 61004, Iraq; basil.jasim@uobasrah.edu.iq (B.H.J.); bilalnaji11@yahoo.com (B.N.A.)

³ Biomedical and Electronics Engineering, Faculty of Engineering and Informatics, University of Bradford, Bradford BD7 1DP, UK; Y.F.Hu@bradford.ac.uk (Y.-F.H.); R.A.A.Abd@bradford.ac.uk (R.A.A.-A.)

* Correspondence: y.i.a.al-yasir@bradford.ac.uk; Tel.: +44-127-423-8047

Abstract: This article presents a novel four-dimensional autonomous fractional-order chaotic system (FOCS) with multi-nonlinearity terms. Several dynamics, such as the chaotic attractors, equilibrium points, fractal dimension, Lyapunov exponent, and bifurcation diagrams of this new FOCS, are studied analytically and numerically. Adaptive control laws are derived based on Lyapunov theory to achieve chaos synchronization between two identical new FOCSs with an uncertain parameter. For these two identical FOCSs, one represents the master and the other is the slave. The uncertain parameter in the slave side was estimated corresponding to the equivalent master parameter. Next, this FOCS and its synchronization were realized by a feasible electronic circuit and tested using Multisim software. In addition, a microcontroller (Arduino Due) was used to implement the suggested system and the developed synchronization technique to demonstrate its digital applicability in real-world applications. Furthermore, based on the developed synchronization mechanism, a secure communication scheme was constructed. Finally, the security analysis metric tests were investigated through histograms and spectrograms analysis to confirm the security strength of the employed communication system. Numerical simulations demonstrate the validity and possibility of using this new FOCS in high-level security communication systems. Furthermore, the secure communication system is highly resistant to pirate attacks. A good agreement between simulation and experimental results is obtained, showing that the new FOCS can be used in real-world applications.

Keywords: adaptive synchronization; chaotic systems; fractional-order; microcontroller; secure communications



Citation: Rahman, Z.-A.S.A.; Jasim, B.H.; Al-Yasir, Y.I.A.; Hu, Y.-F.; Abd-Alhameed, R.A.; Alhasnawi, B.N. A New Fractional-Order Chaotic System with Its Analysis, Synchronization, and Circuit Realization for Secure Communication Applications. *Mathematics* **2021**, *9*, 2593. <https://doi.org/10.3390/math9202593>

Academic Editors: Brenno Caetano Troca Cabella and Carlo Cattani

Received: 22 September 2021

Accepted: 12 October 2021

Published: 15 October 2021

Publisher's Note: MDPI stays neutral with regard to jurisdictional claims in published maps and institutional affiliations.



Copyright: © 2021 by the authors. Licensee MDPI, Basel, Switzerland. This article is an open access article distributed under the terms and conditions of the Creative Commons Attribution (CC BY) license (<https://creativecommons.org/licenses/by/4.0/>).

1. Introduction

In the last few decades, the nonlinear phenomenon in chaos has been widely considered in engineering, sciences, and applied mathematics [1,2]. When a deterministic system exhibits a strange phenomenon of aperiodic trajectories, this is called chaos [3–5]. Chaotic system sensitivity is introduced when the initial conditions and system parameters have a strong influence on chaotic systems; however, even a minor alteration in the starting situation can have a significant impact on the final result [6].

Chaos plays a significant role in many fields, such as biological systems dealing with the human heart and brain [7], protected communication systems [8], smart systems [9], digital signal processing [10], data encryption [11], robotics engineering [12], adaptive control engineering [13], and nonlinear oscillator designs [14]. Recently, several fractional-order systems are proposed to have exhibit chaotic behavior, such as a fractional-order Lotka-Volterra system, a fractional-order Chua Hartley oscillator, a fractional-order Van der

Pol oscillator [15], a fractional-order Lui system [16], a fractional-order Lorenz system [17], and many other systems [18]. The FOCSs are very useful in secure communication and high-level encryption because they exhibit very high complexity in their dynamics.

Fractionality is a branch of mathematics that is an extension of classical calculus. The study of fractional calculus has recently received a lot of attention due to its potential application in different fields [19]. In 1694, Leibniz was asked by L'Hospital if the half order derivative is possible [20]. Representation of a system by a fractional order gives several benefits over its classical integer-order depiction. The fractional-order has transmissible properties, and as a result of that, the core of the real physical system can be more exactly maintained. In addition, the system order " q " can be varied in a range $(0, 1]$ that allows an extension in the system parameter space [21–23].

Fractional calculus has applications in a wide range of engineering and science fields, including fluid mechanics, viscoelasticity, systems' identification, electromagnetics, electrochemistry, biological population models, signal processing, optics, control, analog filters, circuit theory, oscillators, encryption systems, image processing, economics, and chemistry [24–26]. Because fractional-order chaotic models include the fractional-order parameter as well as the original system features, they have more complex dynamical behavior than integer models [27,28].

The chaos synchronization technique is based on the notion that two chaotic systems might evolve on different attractors, but when they are synchronized, they start on various attractors and eventually follow the same course. The synchronization between two systems can be achieved when the trajectories of two systems are matched [29–31]. In chaos systems, the synchronization mechanism plays a significant role in constructing secure communication schemes [32–34]. It can occur between two chaotic systems; one is a master and the driven one is a slave [35,36]. In such applications, the master grants the transmitter, and the slave demonstrates the receiver. Chaotic synchronization was first studied by Yamada and Fujisaka in 1983 [37]. Many control methods have been developed for controlling and synchronizing the fractional-order chaotic systems, such as active control, impulsive control, adaptive control, passive control, and sliding mode control [38].

Many FOCSs have been recognized and used in the security of communication systems. Jialin Hou et al. [39] used the FOCS for proposing image encryption. They use exclusive or (XOR) for encryption algorithm; this encryption system has increased the arbitrariness and improved the encryption speed. The authors developed a traditional integer Chen chaotic system to be a fractional type. Therefore, this system cannot be considered a novel in the subject area. As a result, the encryption system did not provide more high-security performance. Maitreyee Dutta et al. [40] suggested a novel FOCS. The suggested system shows multiple wing chaotic attractors which produce chaos for generating a change in complex attractors by changing only one parameter. A synchronization mechanism based on an adaptive sliding mode controller is used in that system. The proposed system contains a hyperbolic tangent function, which increases the difficulty of its implementation in the real world. On the other hand, our proposed system has not contained such these functions. Thus, it can be implemented simply. Zahra Rashidnejad et al. [41] introduced a finite time synchronization mechanism of two different FOCSs master and slave systems with unknown parameters, disturbances, and uncertainties, where the synchronization was rapidly realized in perfect time. The realization of this investigated synchronization mechanism was not taken into account to prove the feasibility of the application in the real world. An improved cryptosystem image based on FOCS has been proposed by Musheer Ahmad et al. with better performance and appropriateness of the proposed improved algorithm for realizing a robust and strong safe communication scheme [42]. In this work, a control method by Pecora and Carroll (PC) was used to achieve the synchronization mechanism. In our work, we used the adaptive synchronization mechanism. The adaptive synchronization technique has many advantages, including rapid

dynamics responses, good transient performance, and a robust technique for parameter variations, initial conditions, and disturbances.

Several chaotic-based safe communication schemes have been applied over the last few years. Chaotic masking, inclusion, chaotic shift keying, and parameter modulation are the main approaches for exploiting chaotic signals in secure communications [43–45].

In this work, the chaotic masking technique was employed, and a new four-dimensional FOCS was proposed. The proposed FOCS exhibits more complex attractors than an integer regular chaotic system complexity which makes it very suitable for designing high-security communication systems. Since the new FOCS was applied in the secure communication scheme, an adaptive synchronization mechanism was developed between two identical FOCSs, one presented as the master (transmitter) and the other for the slave (receiver). Adaptive control laws were derived based on the Lyapunov approach, which are responsible for attaining master–slave synchronization. Furthermore, an update control rule was developed to estimate an uncertain parameter in the slave side according to the equivalent master side parameter. For verifying the security analysis of the used communication system, histograms and spectrograms were explored. The achieved results were tested and determined by using MATLAB Simulink (MathWorks, Portola Valley, California, United States). Furthermore, a feasible electronic circuit of that new FOCS and its synchronization was realized by Multisim.

The paper's organization is as follows. In Section 2, the fundamental calculus of fractional order is described. In Section 3, the new FOCS are studied by equilibria, eigenvalues, and their chaotic attractors. Their dynamical analysis including the fractal dimension and Lyapunov exponents bifurcation diagrams are investigated in Section 4. For attaining chaos synchronization between two new identical FOCSs with an uncertain parameter in the slave side, adaptive control laws are derived in Section 5. In Section 6, we realize an electronic circuit of the new FOCS. In Section 7, the proposed FOCS and the developed synchronization mechanism are digitally implemented, where the Arduino Due board is used. In Section 8, the suggested FOCS and the synchronization process are applied for encoding and decoding a stream of binary numbers in the master and the slave sides, respectively. In Section 9, histograms and spectrograms are investigated for proving the security analysis of the utilized communication scheme. In Section 10, we conclude this paper.

2. Fractional Order Preliminaries

The history of fractional calculus extends back more than three hundred years [46]. In the development of fractional calculus, there are several fundamentals for differentiation and integration. The popularly used definitions of fractional-order calculations were developed by Grünwald–Letnikov, Caputo, and Riemann–Liouville [47].

Generally, in fractional-order chaotic systems modeling, the Caputo derivative is preferred due to several advantages. Firstly, it takes into account the influences of initial conditions. Secondly, it has a clearer physical meaning. Finally, all fractional operators take the memory effect into account [48,49]. Caputo introduced a definition of the fractional-order derivative (q -order) for a function $f(t)$, as expressed in the following Equation (1) [50].

$${}_t D_t^q f(t) = \begin{cases} \frac{1}{\Gamma(m-q)} \int_{t_0}^t \frac{f^{(m)}(\tau)}{(t-\tau)^{q-m+1}} d\tau; & m-1 < q < n \\ \frac{d^m f(t)}{dt^m}; & q = m. \end{cases} \quad (1)$$

where m is the least integer number, greater than q and $\Gamma(m-q)$ is known as Gamma function is the function that is most used in the fractional calculus, and it is defined in Equation as follows (2) [51]:

$$\Gamma(x) = \int_0^{+\infty} e^{-t} t^{x-1} dt; \quad x > 0 \quad (2)$$

With $\Gamma(1) = 1; \Gamma(0) = +\infty$.

Grunwald–Letnikov approaches the fractional derivative, as demonstrated in the following [52].

$$D^q x(t) = f(x, t) = \lim_{h \rightarrow 0} h^{-q} (-1) \sum_{j=0}^{t/h} (-1)^j \binom{q}{j} x(t - jh) \tag{3}$$

where h is the step size.

The fractional integral operator (J^q) created by Riemann–Liouville for order ($q \geq 0$) of function ($f(t)$) is given by Equation (4) [53].

$$J^q f(t) = \begin{cases} \frac{1}{\Gamma(q)} \int_0^t (t - \tau)^{q-1} f(\tau) d\tau; & q < 0, \\ f(t); & q = 0. \end{cases} \tag{4}$$

3. New Fractional-Order Chaotic System

There are two types of fractional order systems: the commensurate fractional-order system and the incommensurate fractional-order system. The fractional-order values (q_1, q_2, \dots, q_n) of the system equations are equaled in the first type ($q_1 = q_2 = \dots = q_n$), while these values are unequaled in the second type ($q_1 \neq q_2 \neq \dots \neq q_n$) [54].

The FOCS are a special type of nonlinear system; this type of system has the original properties of integer-order chaotic systems and has additional properties, such as high complexity and extreme sudden behavior. Despite the fact that there are a lot of new chaotic systems proposed over the last few years, it is still advantageous for the field of chaos in theoretical and practical areas to develop, discover, and analyze new chaotic systems. This fact is stated in many specialized articles and the article’s references [55–58] are some of these examples. That is because some of the chaotic applications, such as secure communication, require new systems continuously. Here, we proposed a new 4-D FOCS, as demonstrated by the fractional-order dynamic Equation (5).

$$\frac{d^q x}{dt^q} = -ayz, \frac{d^q y}{dt^q} = bxz - c, \frac{d^q z}{dt^q} = x - dz, \frac{d^q w}{dt^q} = kx^3 - w. \tag{5}$$

In Equation (5), x, y, z , and w are the state variables; a, b, d , and k are system positive constant parameters; and q is the fractional-order derivative value. The dynamics which are chaotic attractors, fixed (equilibrium) points, and Lyapunov exponent are investigated for the proposed system. The system (5) shows chaotic actions when selecting parameters $a = 2.5, b = 0.05, c = 1.2, d = 2, k = 0.001$, and the fractional-order $q = 0.9$. Where the initial conditions are $x(0) = 0.1, y(0) = 0.2, z(0) = -1$, and $w(0) = 0.3$. The phase portraits of the proposed system are illustrated in Figure 1. The simulation results for systems (5) were obtained using the Roberto Garrappa method of solving fractional order nonlinear systems, with a step size of ($h = 0.005$) [59].

The equilibrium points (equilibria) of the novel proposed fractional-order chaotic system (5) can be obtained by solving the following nonlinear Equations.

$$\frac{d^q x}{dt^q} = -ayz = 0; \frac{d^q y}{dt^q} = bxz - c = 0; \frac{d^q z}{dt^q} = x - dz = 0; \frac{d^q w}{dt^q} = kx^3 - w = 0 \tag{6}$$

The equilibrium points are determined as given in Table 1. In addition, the eigenvalues consistent with the obtained equilibrium points are calculated by linearizing method (Jacobian matrix of system (5)), as described in Equation (7).

$$J = \begin{bmatrix} 0 & -az & -ay & 0 \\ bz & 0 & bx & 0 \\ 1 & 0 & -d & 0 \\ 3kx^2 & 0 & 0 & -1 \end{bmatrix} \tag{7}$$

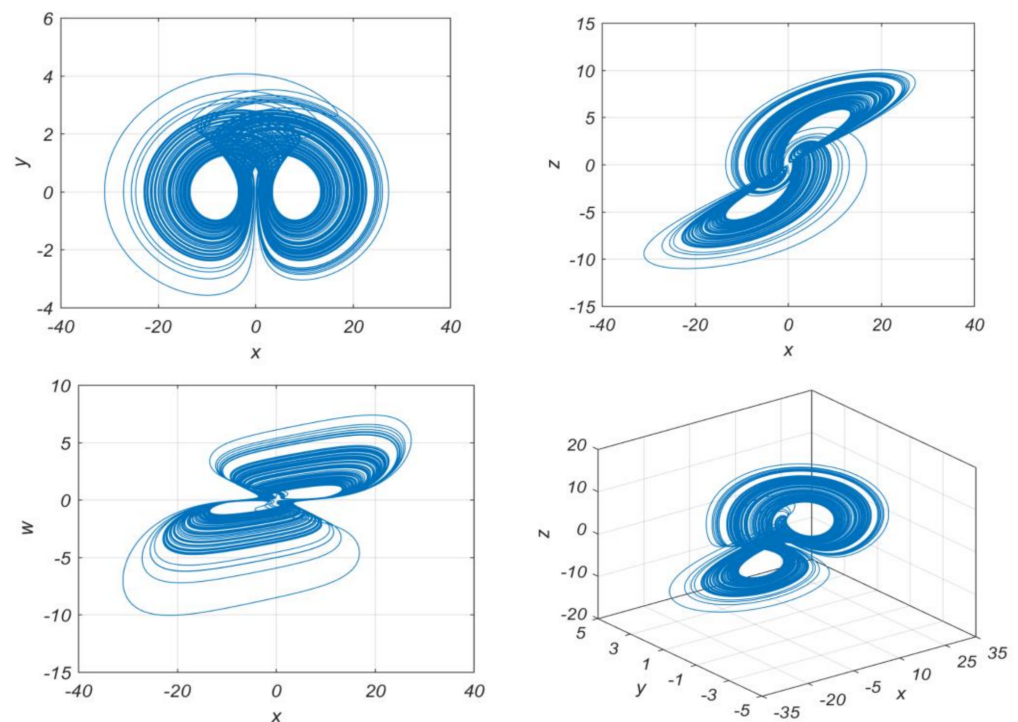


Figure 1. The chaotic attractors in 2D and 3D arrangements.

Table 1. Equilibrium points, consistent eigenvalues, and equilibria class.

No.	Equilibrium Point	Eigenvalues	Equilibria Classification
1	(6.9282, 0, 3.4641, 0.3326)	(−1, 0.2052 + 1.5643i, 0.2052 − 1.5643i, −2.4104)	Saddle focus
2	(−6.9282, 0, −3.4641, −0.3326)	(−1, 0.2052 + 1.5643i, 0.2052 − 1.5643i, −2.4104)	Saddle focus

The equilibrium point in fractional-order systems is stable if the following criterion is met:

$$|arg(\lambda_i)| > q \frac{\pi}{2} ; i = 1, 2, 3 \tag{8}$$

Thus, the equilibria of the new FOCS were classified according to the condition in (8), as illustrated in Table 1 [60]. Generally, a dynamic system with two saddle equilibria connected by heteroclinic exhibits chaos [61]. That is exactly verified in the proposed new nonlinear fractional-order systems.

4. The Dynamical Analysis

Generally, the major dynamical tools that may be used to examine the dynamical behaviors of nonlinear chaotic systems are the fractal dimension, bifurcation diagrams, and Lyapunov exponents [62–64]. The fractal dimension, bifurcation diagrams, and Lyapunov exponents are numerically investigated using MATLAB.

4.1. Fractal Dimension

The basic parameter for describing self-similar patterns and processes is the fractal dimension. The concept of fractal dimension is useful in describing natural objects because it indicates their degree of complexity [65]. There are several approaches to calculate the fractal dimension. For example, Higuchi’s method, the rescaled range method, Renyi’s entropy, and Katz’s method. Higuchi’s fractal dimension (HFD) is a popular nonlinear measure for signal analysis and it is a time-domain signal complexity metric [66].

Higuchi’s method for calculating the fractal dimension of a signal or function is explained following [67]. An epoch with N number of samples of the signal is represented by $x(1), x(2), \dots, x(N)$. K is new sub-epochs that are constructed from this original epoch and represented by X_m^k , where sub-epoch is described by the following equation.

$$X_m^k = \{x(m), x(m+k), x(m+2k), \dots, x(m + \text{int}[(N-k)/k]k); m = 1, 2, \dots, k \quad (9)$$

$$k = 1, 2, \dots, k_{max}$$

In Equation (9) $m, k, \text{int}(\cdot)$, and k_{max} are the initial time, the time interval, integer real part number, and a free parameter, respectively.

The average length $L_m(k)$ for each of the sub-epochs constructed can be calculated: as:

$$L_m(k) = \frac{1}{k} \left[\left(\sum_{i=1}^{\text{int}[(N-m)/k]} |x(m+ik) - x(m+(i-1)k)| \right) \frac{N-1}{(\text{int}[(N-m)/k]k)} \right] \quad (10)$$

The mean of the k values is used to calculate the length of the epoch $L(k)$ for the time interval k as follows.

$$L(k) = \frac{1}{k} \sum_{m=1}^k L_m(k) \quad (11)$$

Finally, Higuchi’s fractal dimension can be estimated as.

$$HFD = \frac{\ln(L(k))}{\ln(1/k)} \quad (12)$$

The choice of the free parameter k_{max} is critical in HFD estimation. In our work, HFD values were calculated for various k_{max} values with N ranging from 500 to 10,000, as shown in Figure 2. A smooth signal’s HFD value (for example, a low-frequency sine wave and linear) was estimated to be 1. The HFD of random white noise or more complex signals was calculated to be ≈ 2 . Because it is a numerical approximation of the fractal dimension, the calculated HFD values may be slightly greater than 2 [68]. Therefore, it can be noted from Figure 2 that the suggested FOCS exhibits very complex dynamical behavior.

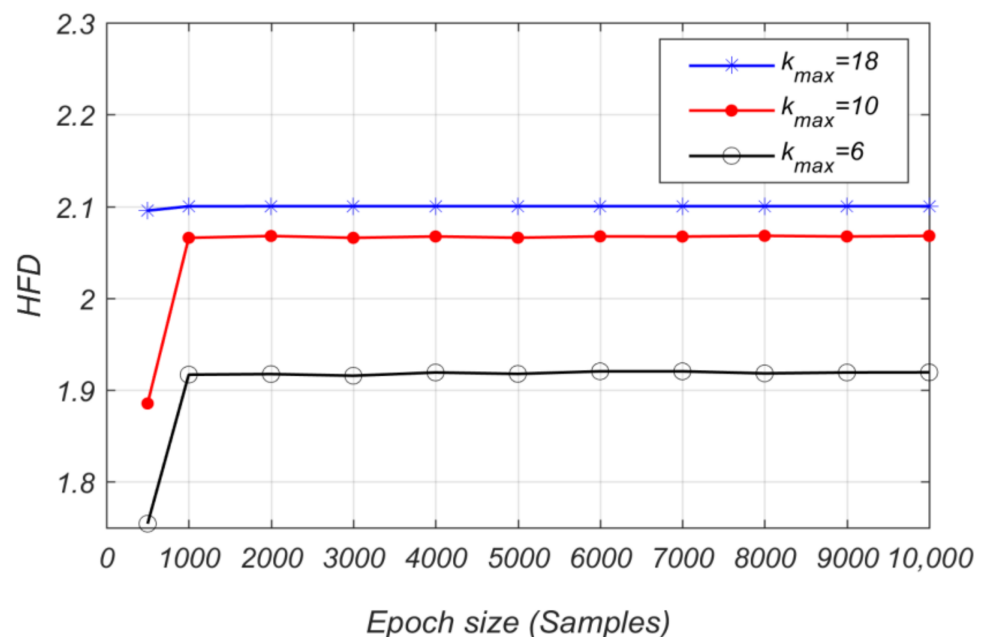


Figure 2. The HFD of the suggested FOCS.

4.2. Bifurcation Diagrams

It can be proven that the proposed system exhibits the chaoticity phenomena by the bifurcation diagrams [69]. For the proposed system, the bifurcation diagram is numerically calculated in two cases, one with respect to parameter d of the system in (5), and the other case versus the fractional-order derivative value (q).

Figure 3a shows the system bifurcation diagram against the parameter d , where the parameters are selected as $a = 2.5$, $b = 0.05$, $c = 1.2$, $k = 0.001$, and the fractional order $q = 0.9$ with initial conditions $x(0) = 0.1$, $y(0) = 0.2$, $z(0) = -1$, and $w(0) = 0.3$. Figure 3b shows the system bifurcation diagram against the fractional order (q) with the same values in Figure 3a, except the parameter $d = 2$. The new system exhibits chaos in range $d \in [0.745, 2]$ and, for the fractional-order derivative value (q), the range is $[0.896, 1]$. As seen in Figure 3, the new proposed system exhibits a variety of bifurcation topological patterns.

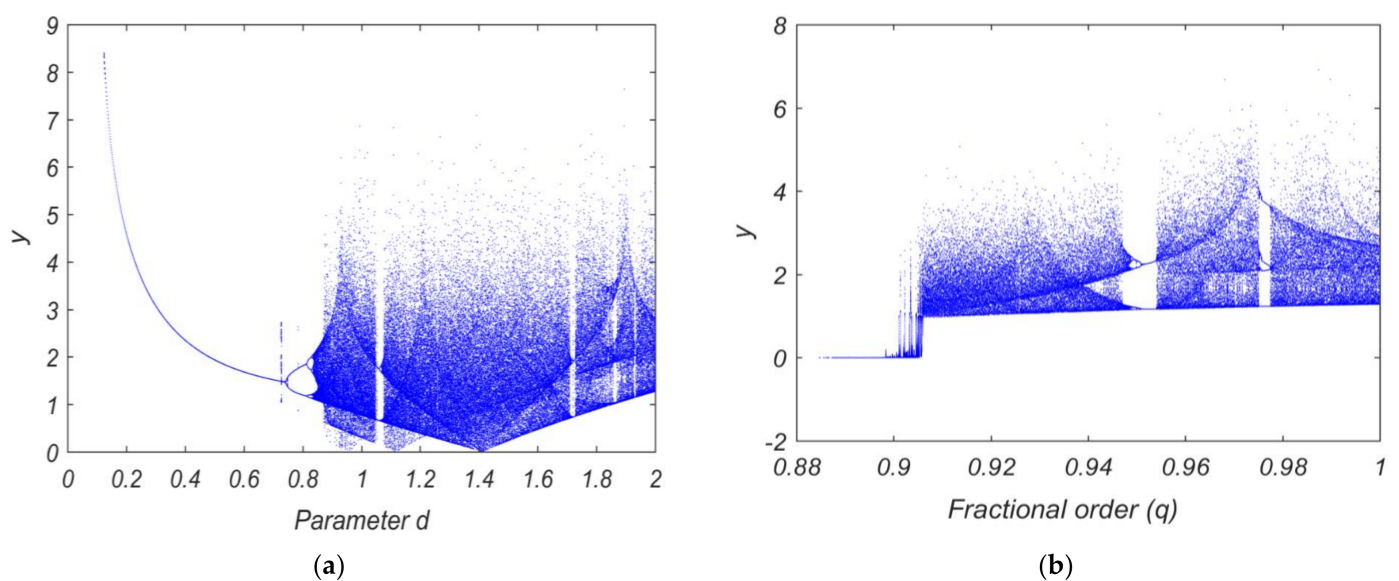


Figure 3. The bifurcation diagram of the proposed FOCS with respect to: (a) Parameter d ; (b) Fractional-order derivative value.

4.3. Lyapunov Exponents

Lyapunov exponents are calculated and strongly indicate that the new system exhibits the chaoticity phenomena. At least one positive Lyapunov exponent in nonlinear dynamic systems ensures that these systems display chaos [70,71]. For the suggested system, the Lyapunov exponents are numerically determined, as shown in Figure 4. The Lyapunov exponents are obtained as: $Le1 = 0.1585$, $Le2 = -0.0001$, $Le3 = -1.0366$, and $Le4 = -2.2034$. Thus, the proposed FOCS exhibits chaotic performance because one of the Lyapunov exponents is positive.

Moreover, Lyapunov exponents are determined when the fractional-order derivative value is changed to $q \in [0.88, 1]$, as illustrated in Figure 5. The system parameters utilized in this calculation are the same as those used in the first Lyapunov exponent's computations. As shown in Figure 5, the Lyapunov exponents are $Le1 = 0.6461$, $Le2 = 0.1654$, $Le3 = -0.1223$, and $Le4 = -0.7161$, which indicates a chaotic phenomenon in our proposed system.

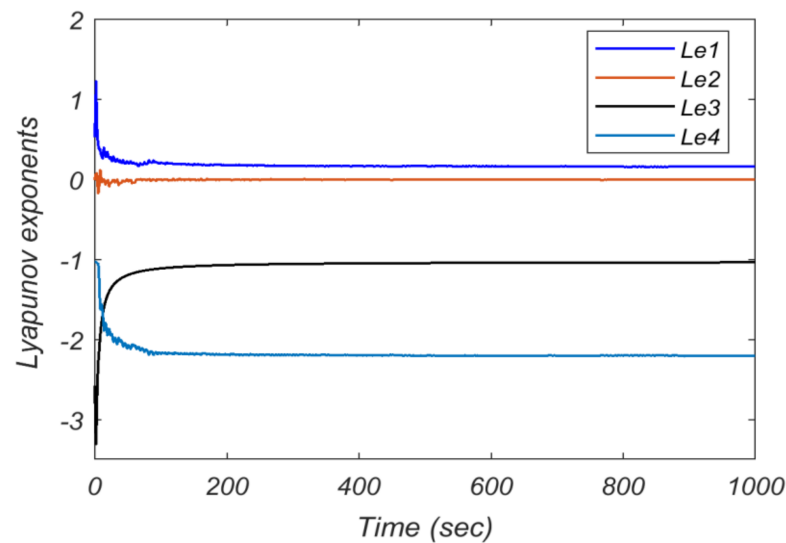


Figure 4. Lyapunov exponents with parameters $a = 2.5$, $b = 0.05$, $c = 1.2$, $d = 2$, $k = 0.001$, and the fractional order $q = 0.9$ with initial conditions $x(0) = 0.1$, $y(0) = 0.2$, $z(0) = -1$, and $w(0) = 0.3$.

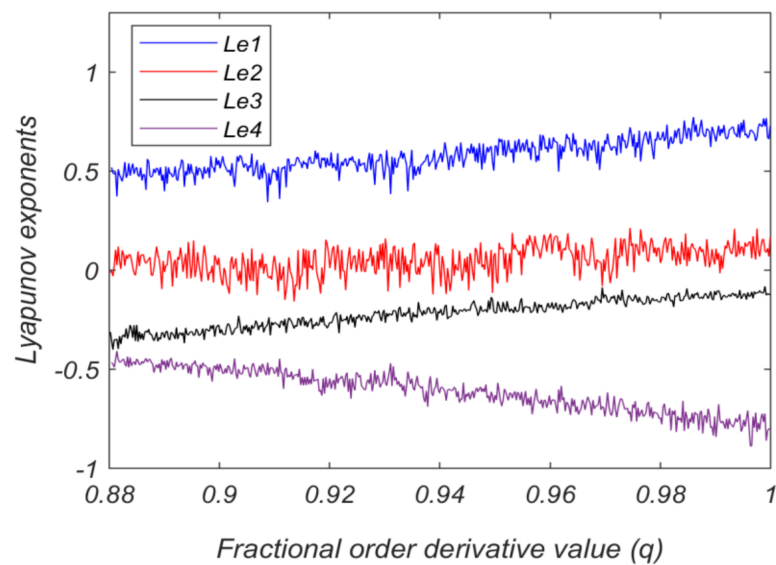


Figure 5. Lyapunov exponents corresponding to the fractional-order derivative value (q).

5. Adaptive Synchronization

Practically, the two important ways to utilize chaos are chaos control and synchronization techniques [72]. The chaos synchronization has received much attention; this is because the secure communication schemes primarily depend on the synchronization between the transceivers [73,74]. Researchers have introduced many chaos control and synchronization techniques, as listed in the introduction section.

In this work, an adaptive synchronization mechanism is developed for synchronizing two identical new FOCSs; one acts the master (transmitter side) and the other acts the slave (receiver side). Based on the Lyapunov method, adaptive control laws were derived, which are responsible for achieving the synchronization between the master and the slave. Furthermore, an update control law was designed for estimating the single uncertain parameter in the slave side, corresponding to the equivalent master parameter.

5.1. Adaptive Control Law Design

In this section, we derive the adaptive and update control laws. The drive system (master) and controlled system (slave) dynamics are named as in Equations (13) and (14), respectively:

$$\frac{d^q x_m}{dt^q} = -ay_m z_m; \frac{d^q y_m}{dt^q} = bx_m z_m - c; \frac{d^q z_m}{dt^q} = x_m - d_1 z_m; \frac{d^q w_m}{dt^q} = kx_m^3 - w_m \tag{13}$$

$$\frac{d^q x_s}{dt^q} = -ay_s z_s + u_1 + u_1; \frac{d^q y_s}{dt^q} = bx_s z_s - c + u_2; \frac{d^q z_s}{dt^q} = x_s - d_2(t)z_s + u_3; \frac{d^q w_s}{dt^q} = kx_s^3 - w_s + u_4 \tag{14}$$

As shown in Equation (14), the adaptive controllers to be designed are $u_1, u_2, u_3,$ and $u_4,$ and $d_2(t)$ is the uncertain parameter in the slave system to be estimated. The synchronization errors between systems (13) and (14) can be defined in the following equation.

$$e_1 = x_s - x_m; e_2 = y_s - y_m; e_3 = z_s - z_m; e_4 = w_s - w_m \tag{15}$$

Therefore, the error dynamics can be obtained by Equations (16)–(19).

$$\frac{d^q e_1}{dt^q} = a(y_m z_m - y_s z_s) + u_1 \tag{16}$$

$$\frac{d^q e_2}{dt^q} = b(x_s z_s - x_m z_m) + u_2 \tag{17}$$

$$\frac{d^q e_3}{dt^q} = e_1 - d_2 e_3 - e_d z_m + u_3 \tag{18}$$

$$\frac{d^q e_4}{dt^q} = k(x_s^3 - x_m^3) - e_4 + u_4 \tag{19}$$

In Equation (18), the master–slave parameter estimation error $e_d(t)$ is given in Equation (20).

$$e_d = d_2(t) - d_1 \tag{20}$$

As a result, the parameter error dynamics can be obtained in Equation (21).

$$\dot{e}_d = \dot{d}_2(t) \tag{21}$$

The Lyapunov approach is used to derive the update law that is responsible for estimating the uncertain parameter in the slave side corresponding to the equivalent parameter of the master. The quadratic Lyapunov function is determined in Equation (22).

$$V(e_1, e_2, e_3, e_4, e_d) = \frac{1}{2} (e_1^2 + e_2^2 + e_3^2 + e_4^2 + e_d^2) \tag{22}$$

Then, differentiating Equation (22) with respect to time, yields Equation (23).

$$\dot{V} = \left(e_1 \frac{d^q e_1}{dt^q} + e_2 \frac{d^q e_2}{dt^q} + e_3 \frac{d^q e_3}{dt^q} + e_4 \frac{d^q e_4}{dt^q} + e_d \dot{e}_d \right) \tag{23}$$

Replacing the dynamic errors from Equations (16)–(21) in Equation (23) gives:

$$\begin{aligned} \dot{V} = & (e_1(a(y_m z_m - y_s z_s) + u_1) + e_2(b(x_m z_m - x_s z_s) + u_2) + e_3(e_1 \\ & - d_2 e_3 - e_d(t)z_m + u_3) + e_4(k(x_s^3 - x_m^3) - e_4 + u_4) \\ & + (d_2(t) - d_1)\dot{d}_2(t)) \end{aligned} \tag{24}$$

The feedback adaptive controller functions have been designed, as named in Equation (25) based on Lyapunov theory for stability. Where many methods can be used for designing similar controllers, as in [75,76].

$$\begin{aligned}
 u_1 &= -k_1 e_1 - (1 + a(y_m z_m - y_s z_s)) e_1; u_2 \\
 &= -k_2 e_2 - (1 + b(x_m z_m - x_s z_s)) e_2; u_3 \\
 &= -k_3 e_3 - e_1 + d_2 e_3 - e_3; u_4 = -k_4 e_4 - k(x_s^3 - x_m^3) e_4
 \end{aligned}
 \tag{25}$$

where k_1, k_2, k_3 and k_4 , are positive constants. Additionally, the updating law that is responsible for updating the uncertain slave parameter is obtained in Equation (26):

$$\dot{e}_d = z_m e_3 \tag{26}$$

Finally, by substituting the feedback adaptive controller functions described by Equation (25) and the update law named by Equation (26) in Equation (24), we get Equation (27).

$$\dot{V} = -k_1 e_1^2 - k_2 e_2^2 - k_3 e_3^2 - k_4 e_4^2 \tag{27}$$

A negative definite function is shown in Equation (27) [77]. Therefore, for any initial conditions, the synchronization state errors converge to zero exponentially with respect to time. In addition, the estimated slave parameter exponentially aligned with the equivalent master parameter. As a result, the established synchronization technique’s asymptotic global stability is guaranteed.

5.2. Numerical Simulation

For the numerical simulations, MATLAB software is used for simulating this adaptive synchronization mechanism between the two identical FOCSs (13) and (14). In the synchronization simulation, the parameters of the new FOCSs are chosen as $a = 2.5, b = 0.05, c = 1.2, d_1 = 2, d_2(t)$ is uncertain, $k = 0.001$, and the fractional order $q = 0.9$. Where the initial conditions for the master are $x_m(0) = 0.1, y_m(0) = 0.2, z_m(0) = -1$, and $w_m(0) = 0.3$. For the slave, they are $x_s(0) = 0.2, y_s(0) = 0, z_s(0) = 0.1$, and $w_s(0) = -1$.

The state variables synchronization of the identical novel FOCSs is shown in Figure 6. The 3-D projections of phase portrait for the master–slave synchronization are demonstrated in Figure 7, where the synchronization process was simulated for 12 s only. Figure 8 confirms the convergence of the synchronization errors e_1, e_2, e_3 , and e_4 which exponentially tend to zero with respect to time. Figure 9 illustrates the parameter estimation, where parameter $d_2(t)$ in the slave side is exponentially converging to the equivalent parameter value ($d_1 = 2$) on the master side.

Furthermore, the slave was subjected to disturbances for testing the robustness and disturbance rejection capabilities of the developed synchronization mechanism. Where the disturbances $\delta_1(t), \delta_2(t), \delta_3(t)$, and $\delta_4(t)$ were inserted into the slave state variables, as shown in the following equation.

$$\begin{aligned}
 \frac{d^q x_s}{dt^q} &= -a y_s z_s + u_1 + \delta_1(t); \frac{d^q y_s}{dt^q} = b x_s z_s - c + u_2 - a y_s z_s + u_1 + \delta_2(t); \\
 \frac{d^q z_s}{dt^q} &= x_s - d_2(t) z_s + u_3 - a y_s z_s + u_1 + \delta_3(t); \\
 \frac{d^q w_s}{dt^q} &= x_s - d_2(t) z_s + u_3 - a y_s z_s + u_1 + \delta_4(t)
 \end{aligned}
 \tag{28}$$

The developed synchronization mechanism shows a good robustness against disturbances as confirmed in Figure 10. The disturbances are chosen as $\delta_1(t) = 0.15 \sin(4t), \delta_2(t) = 0.08 \sin(4t), \delta_3(t) = 0.1 \sin(4t)$, and $\delta_4(t) = 0.13 \sin(4t)$. Where these disturbances were subjected to slave states at a time of 25 s.

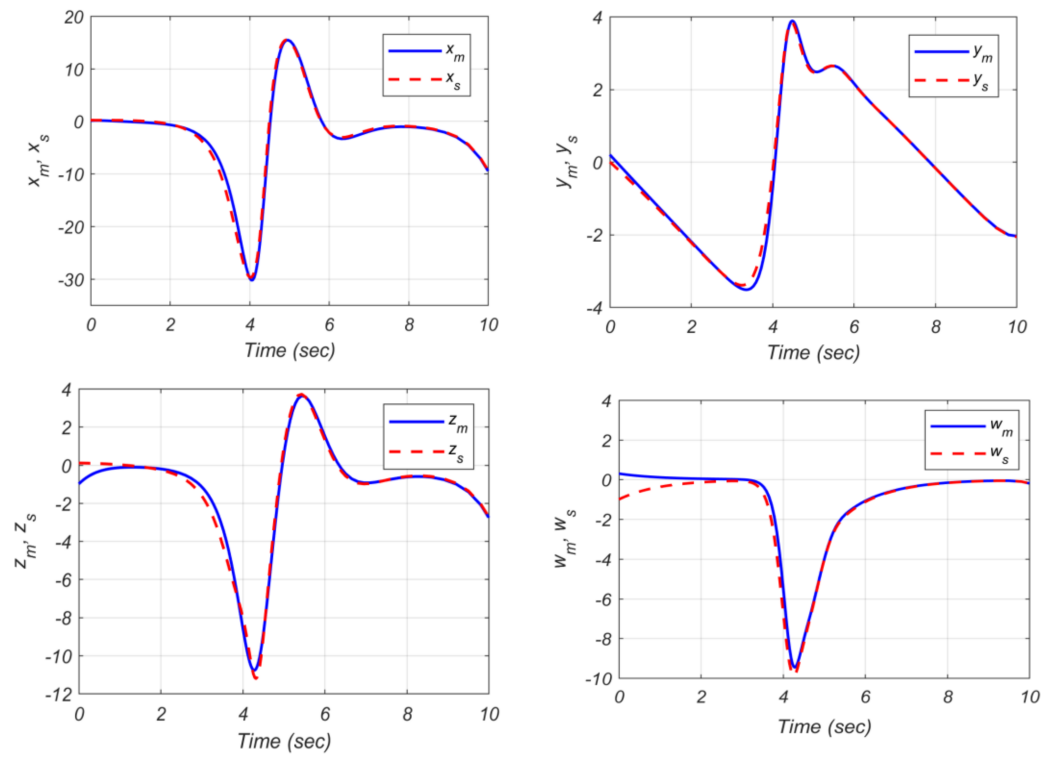


Figure 6. State variables synchronization of the two identical FOCSs.

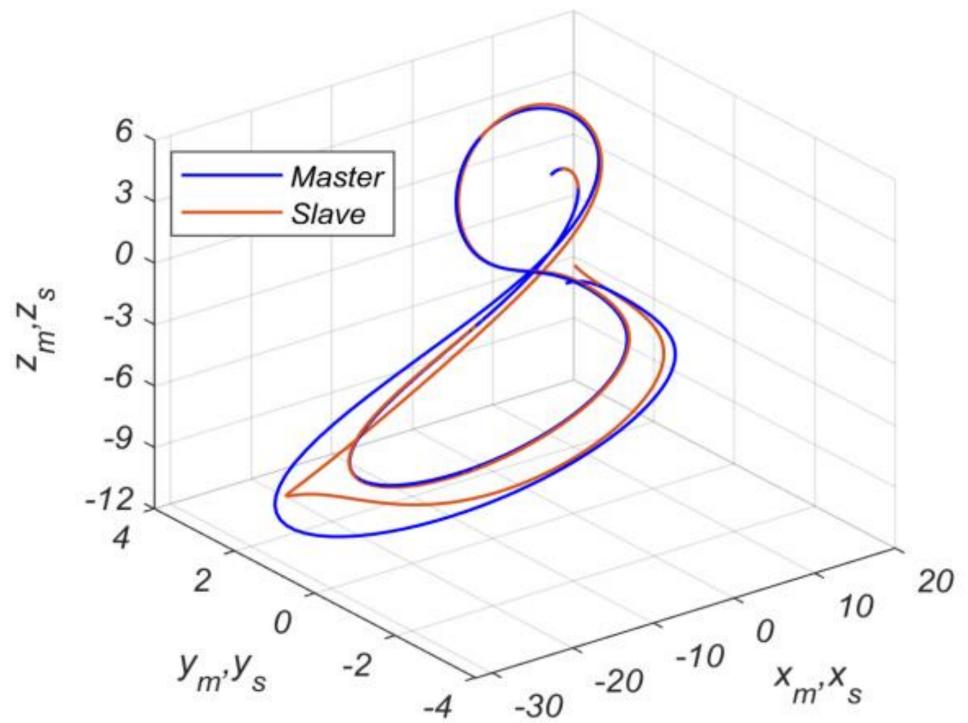


Figure 7. Three-dimensional phase portrait showing the synchronization performance of the master and response slave systems.

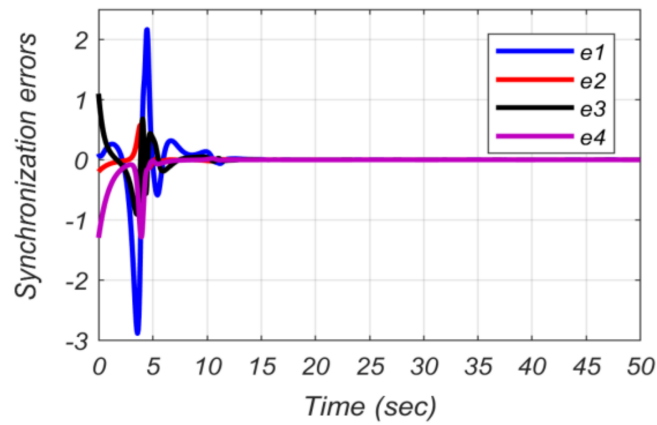


Figure 8. The synchronization errors e_1 , e_2 , e_3 , and e_4 .

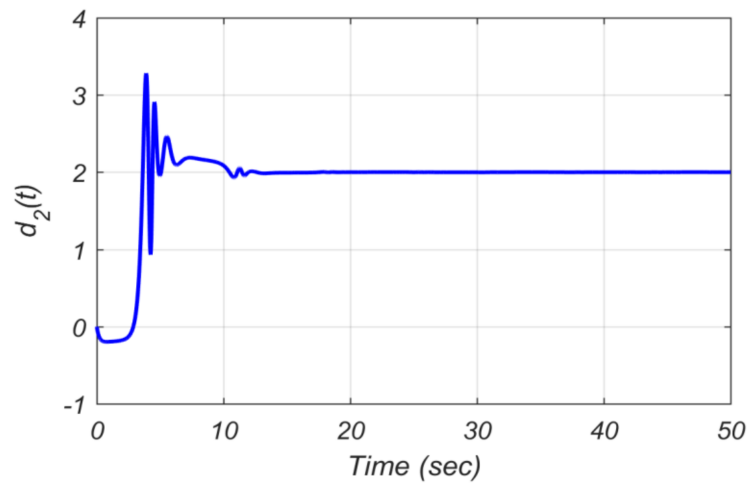


Figure 9. Slave parameter $d_2(t)$ estimation.

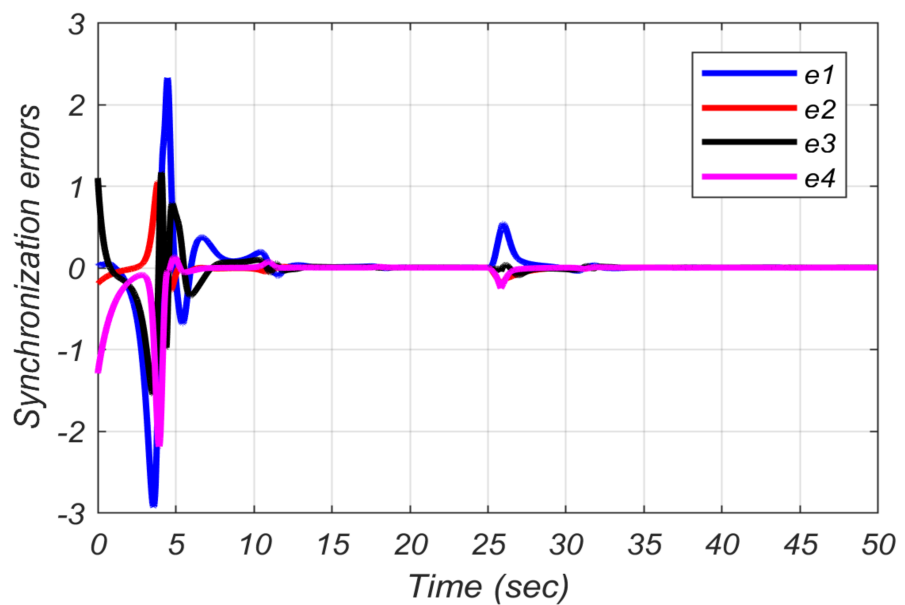


Figure 10. The synchronization errors e_1 , e_2 , e_3 , and e_4 , the slave subjected to disturbances at a time of 25 s.

6. Electronic Circuit Realization

In real-world applications, there are no electronic circuit devices that can reproduce the fractional-order operator; therefore, there are challenges in realizing the fractional-order transfer functions. Ahmed and Sprott introduced the approximation of $1/s^{0.9}$, as in Equation (29) [78].

$$\frac{1}{s^{0.9}} = \frac{2.2675(s + 1.292)(s + 215.4)}{(s + 0.01292)(s + 2.154)(s + 359.4)} \quad (29)$$

The electrical component that exhibits fractional order impedance features is called a fractance [79]. In realization of these devices, the classical integer integrator (op-amp integrator) can be used by replacing the capacitor with the fractance that is equivalent to the designed fractional-order operator. Therefore, the fractional-order integrator is obtained. The realization of the proposed FOCS and its synchronization by an electronic circuit are verified for confirming the feasibility of using the new FOCS in real applications.

In the circuit design of the FOCS, for the order $q = 0.9$, the key idea is how to design the circuit of $1/s^{0.9}$. The chain fractance realization corresponding to $1/s^{0.9}$ is shown in Figure 11 [80].

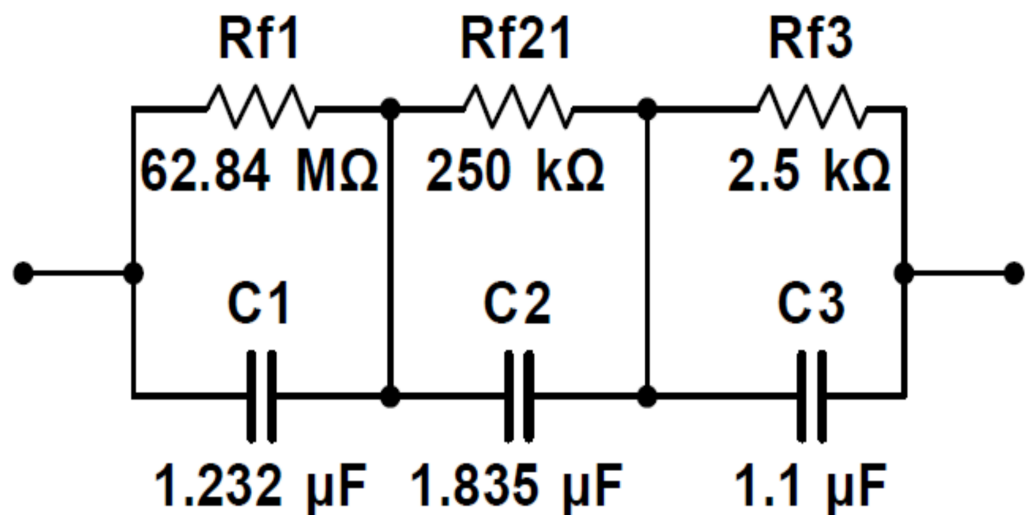


Figure 11. Chain fractance cell (CFC) of $1/s^{0.9}$.

So, based on the fractional-order frequency domain calculation function in Equation (29), it is easy to construct a FOCS electronic circuit. It needs simple elements, such as operational amplifiers and resistors, as well as the chain fractance element that is shown in Figure 11 above. Figure 12 illustrates the electronic circuit schematic diagram for realizing the proposed FOCS. In Figure 13, the phase portraits of the chaotic attractors for the realized electronic circuit of the new FOCS are obtained. Additionally, the adaptive synchronization mechanism of two FOCSs is verified by electronic circuits. The results of electronic circuits of the master–slave system synchronization are shown in Figure 14. Circuit simulation outputs (see Figure 13) show good qualitative matching with the numerical simulations (see Figure 1).

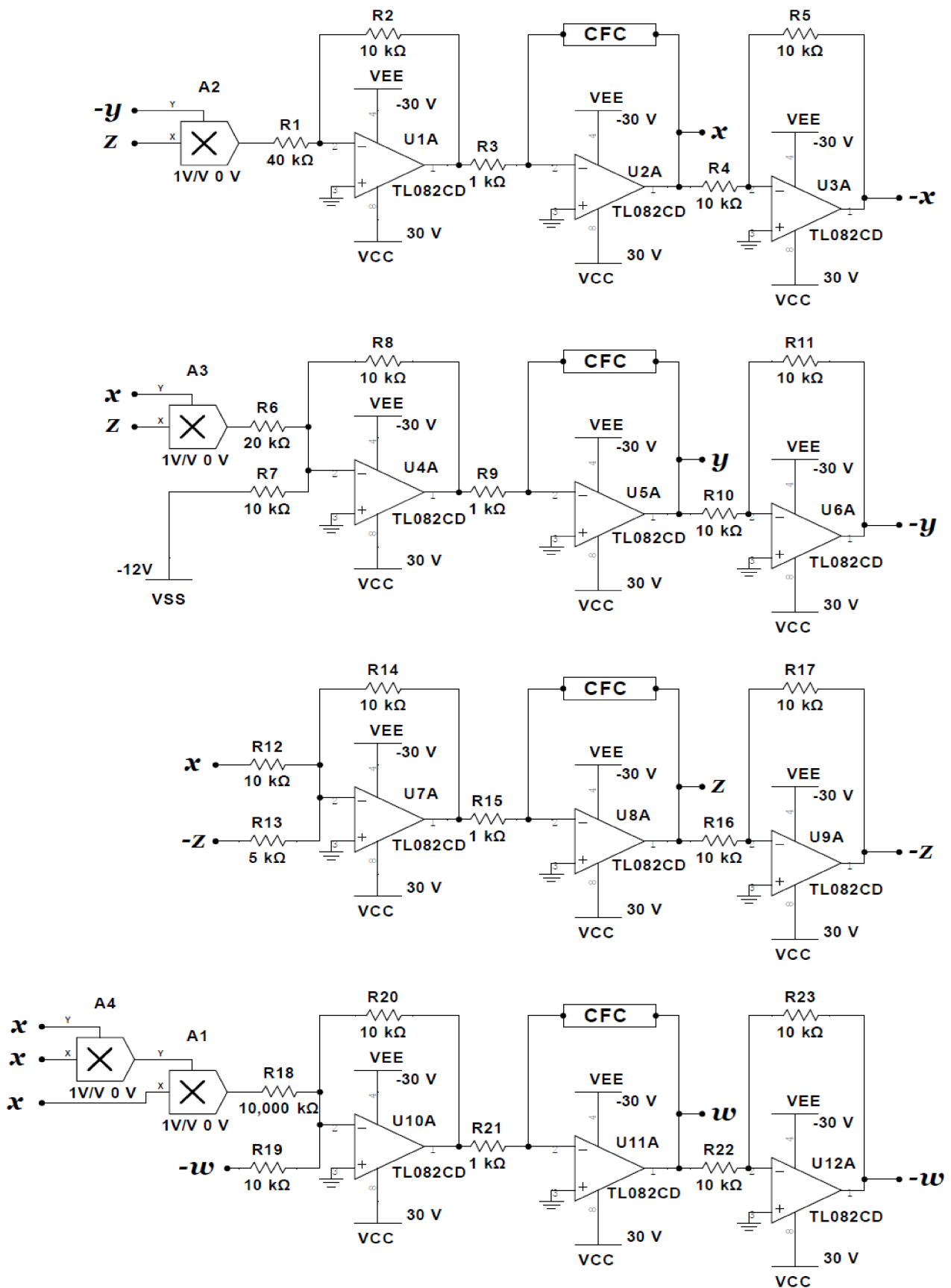


Figure 12. Electronic scheme of the proposed FOCS.

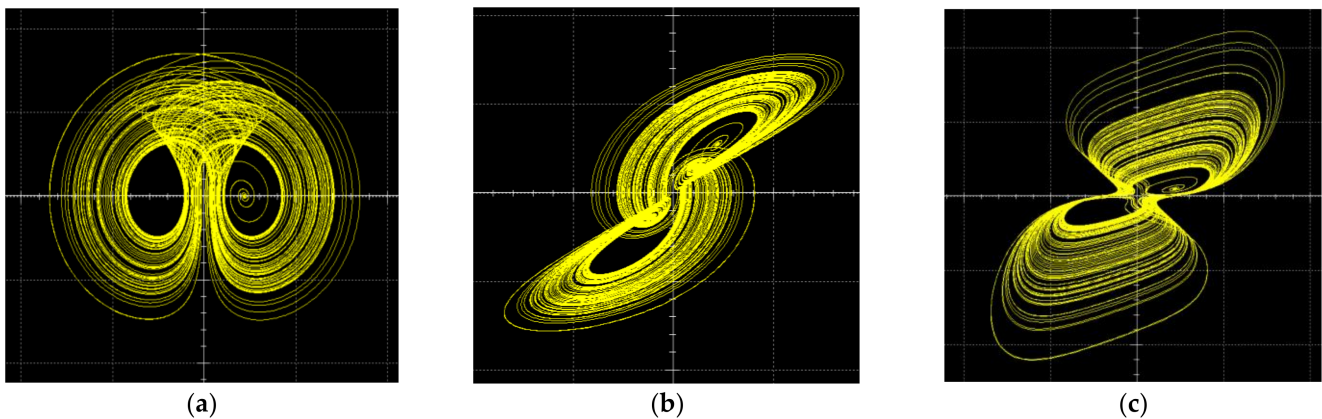


Figure 13. Electronic circuit phase portraits with: (a) $x(5V/Div)$ - $y(2V/Div)$ plane; (b) $x(5/Div)$ - $z(2V/Div)$ plane; (c) $x(5V/Div)$ - $w(1V/Div)$ plane.

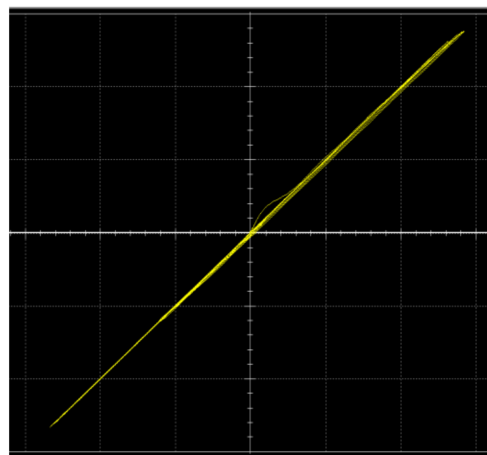


Figure 14. The synchronization circuit experimental result, x_m (2V/Div) state verse x_s (2V/Div) state.

7. Microcontroller Implementation

The main purpose of this section is to prove the implementation of the new FOCS and the developed synchronization mechanism in real-world applications. Fractional-order chaotic systems can be implemented in hardware using several embedded devices, such as Raspberry Pi, microcontrollers, DSP boards, FPGA boards, and analog electronics circuit implementation, as described in Section 6.

In our work, we used a microcontroller (Arduino Due) to implement the new FOCS system in Equation (5) using a discrete technique, as described in [81]. The Arduino Due is a digital board that features an Atmel SAM3X8E processor and an ARM Cortex-M3 processor. It has a structure that is suited for executing complex arithmetic operations. It features the following characteristics in a nutshell: 4 UARTs, 2 DAC (digital to analog), power jack 2 TWI, SPI header, JTAG header, 32-bit ARM core microcontroller, 84 MHz clocks, 54 digital input/output pins, 12 analog inputs, USB OTG capable connection, 2 DAC (digital to analog), and power jack 2 TWI.

The following are the main benefits of using this microcontroller: 12-bit resolution for its two peripherals, DAC0 and DAC1, and a lower cost when compared with FPGAs or DSP boards. The Arduino IDE uses an Arduino-specific programming language, which is comparable with C++ to program the ARM microcontroller via the native USB port (serial port) [82]. Figure 15 shows the Arduino Due microcontroller setup for implementing the new FOCS.

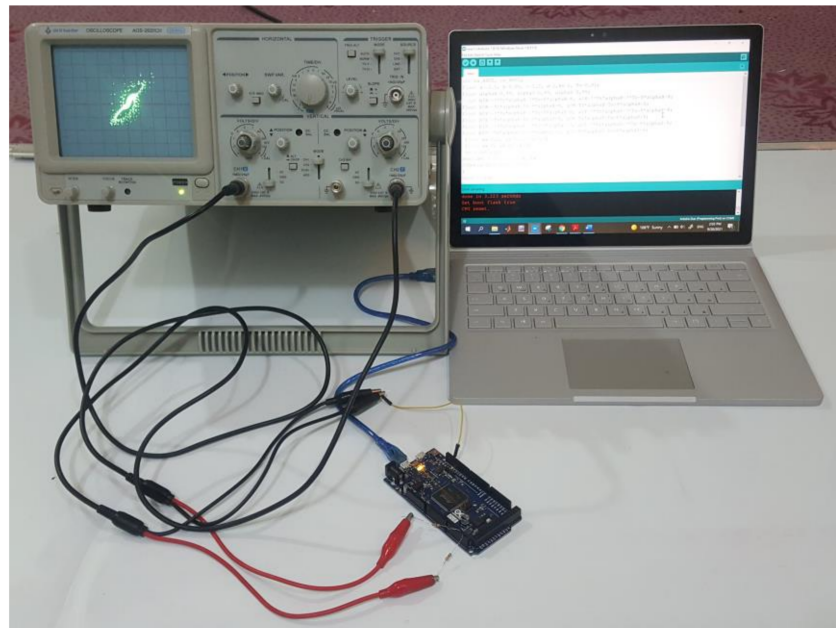


Figure 15. The microcontroller setup of the new FOCS implementation.

For the experimental test, the FOCS parameters are selected as $a = 2.5$, $b = 0.05$, $c = 1.2$, $d = 2$, $k = 0.001$, and the fractional-order $q = 0.9$ with the following initial conditions: $x(0) = 0.1$, $y(0) = 0.2$, $z(0) = -1$, and $w(0) = 0.3$. The ADC0 and DAC1 are utilized to generate phase portraits of chaotic attractors by analog oscilloscope for the system described by Equation (5), as shown in Figure 16.

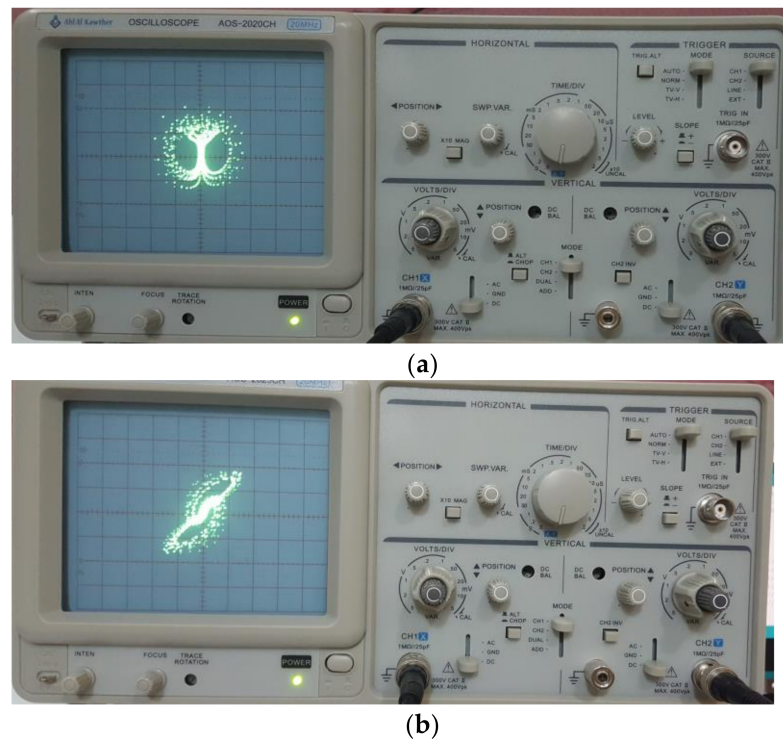
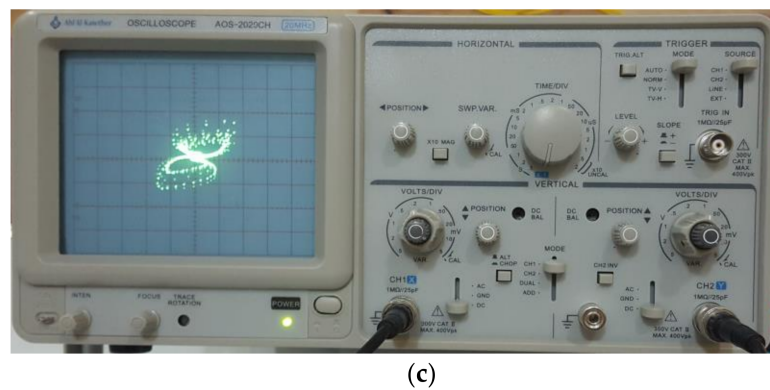


Figure 16. Cont.



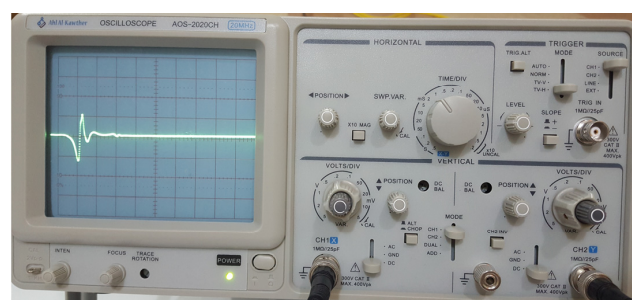
(c)

Figure 16. Two-dimensional phase portraits of the new FOCS system obtained from the microcontroller: (a) $x-y$; (b) $x-z$; (c) $x-w$.

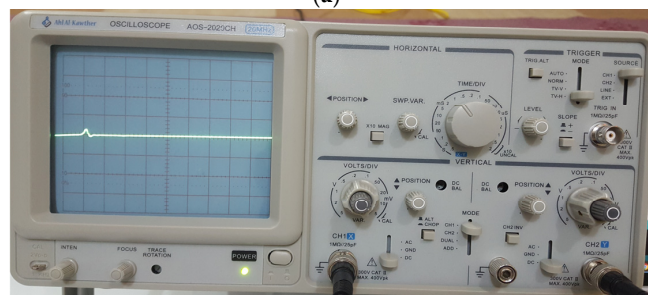
Because the digital to analog converters (DAC0 and DAC1) on the microcontroller operate between 0.5 and 2.7 V, the amplitudes of the MATLAB simulation and the Arduino Due experimental results for the state variables (system trajectories) of the proposed FOCS will be different. To reach the same amplitude values as the estimated numerical simulations, an external operational amplification step would be required.

Furthermore, the developed synchronization technique was digitally implemented and tested by the Arduino Due board. The main advantages satisfied when the synchronization process is implemented by that microcontroller type include its open source, the simplicity of the implementation, and the lower cost when compared with other above-mentioned devices.

Figure 17 shows the behavior of the synchronization error obtained experimentally in the oscilloscope when compared to the synchronization errors obtained by numerical simulation in Figure 8. It is clear that they have the same behavior, implying that the developed adaptive master–slave synchronization process can be digitally implemented by Arduino Due boards. Where the FOCS parameters, initial conditions, and the fractional-order derivative value are used as selected in the numerical simulation, as described by Section 5.2.



(a)



(b)

Figure 17. Cont.

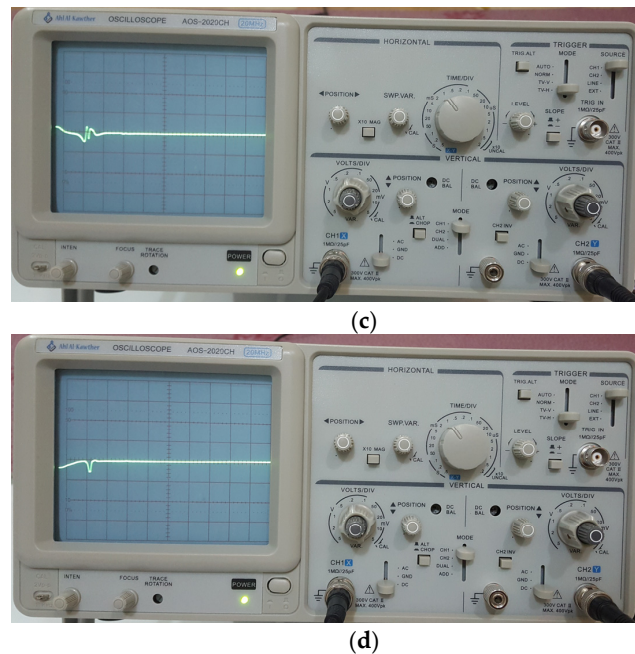


Figure 17. The experimental results of the synchronization error evaluation: (a) e_1 ; (b) e_2 ; (c) e_3 ; (d) e_4 .

Figure 18 shows the experimental results of parameter estimation, where the slave side’s parameter $d_2(t)$ is exponentially convergent to the master side’s equivalent parameter value ($d_1 = 2$).

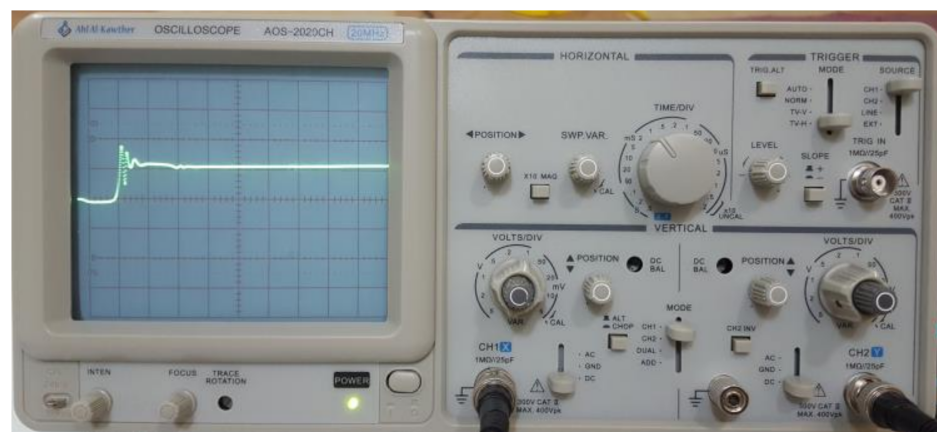


Figure 18. The experimental results estimation of the uncertain slave parameter $d_2(t)$.

8. Application in Secure Communication

Due to the broadband spectrum of chaotic signals, it is very suitable to use these systems in secure communication applications [83]. The above designed adaptive synchronization technique is applied in secure communication arrangements. The chaotic masking technique has the advantage of being simple and easy to implement by electronic circuits [84]. Therefore, this technique was used in our work. Figure 19 depicts the block diagram of the suggested secure communication scheme based on an adaptive synchronization technique between two new FOCSS. As mentioned above, the overall construction is mainly composed of two parts: the derived end (master or transmitter) and controlled end (slave or receiver).

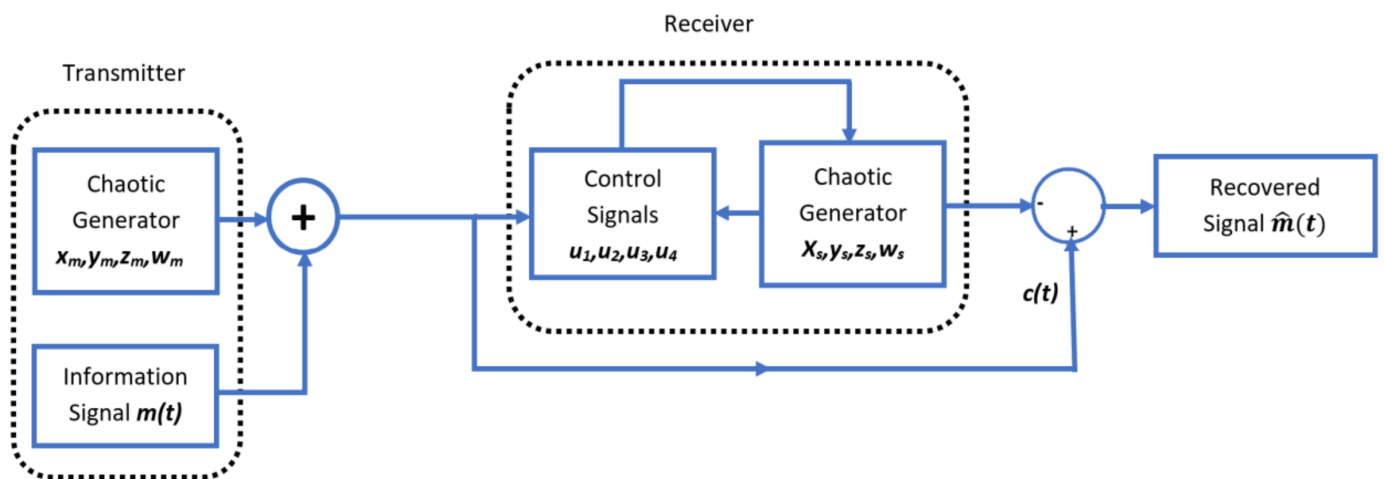


Figure 19. The block diagram of secure communication based on the FOCS.

As shown in Figure 19, the information signal $m(t)$ is added to the generated chaotic signal from the transmitter side, which results in the transmitted signal $c(t)$ being encoded. Thanks to the synchronization, at the receiver side, the same chaotic signal is created at the transmitter side. Then, the original information signal can be recovered by subtracting the chaotic signal from the encoded signal.

On the transmitter side, the information signal is added to the generated chaotic signal as in Equation (30).

$$c(t) = m(t) + w_m(t) \tag{30}$$

On the other hand, at the receiver, the original information signal $\hat{m}(t)$ can be retrieved by subtracting the receiver chaotic signal from the transmitted signal as in Equation (31). Figure 20 illustrates the simulation results of a secure communication scheme based on FOCS, where a noiseless channel is assumed.

$$\hat{m}(t) = c(t) - w_s(t) \tag{31}$$

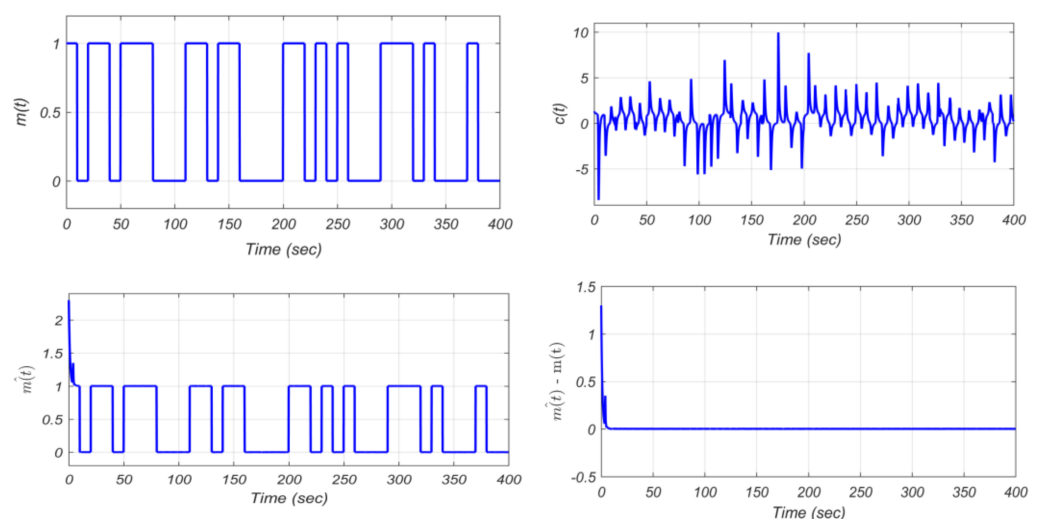


Figure 20. Secure communication scheme signals.

In the real world, a certain amount of noise is introduced to the transmitted signals in the real channel. Therefore, additive white Gaussian noise (AWGN) with various signal-to-

noise ratio (SNR) values is considered in this work. The white Gaussian noise symbolled by $n(t)$ displays in the transmitted signal as follows.

$$c(t) = m(t) + w_m(t) + n(t) \quad (32)$$

The obtained results of the recovered signal with SNR up to 30 dB and 35 dB are shown in Figure 21a,b respectively. As seen from Figure 21, the distortion noticed within the recovered signal is further increased in the noise level (decrease in the SNR).

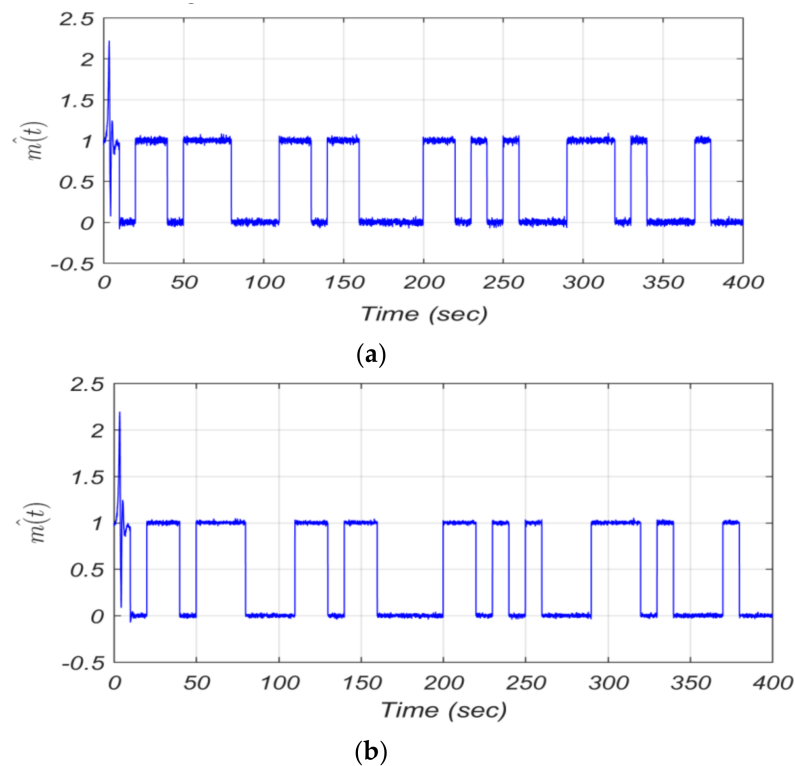


Figure 21. The recovered signal with AWGN noisy channel: (a) SNR = 30 dB; (b) SNR = 35 dB.

9. Security Analysis

It is well known that a secure communication system should be resistant to pirate attacks. Histograms and spectrograms were used in this work to demonstrate the high-security performance of the applied communication system in resisting pirate attacks. This is because the presence of noise increases the difficulty of detecting a signal. Therefore, the security analysis of the applied communication system was investigated, with the assumption of a noiseless channel.

9.1. Histogram Analysis

The histogram of any signal is a graph that depicts the distribution of signal intensity levels [85]. Histogram analysis can be used to evaluate the statistical analysis of the original information and the encrypted versions [86]. Because an information signal is a stream of binary numbers, it only has two clear intensities. As a result, the histogram will display two levels indicating the signal distribution among the intensity values. On the other hand, the histogram of encrypted signal displays many different levels of its intensities.

The histogram of an encrypted signal should be statistically and visually different from the histogram of the original signal. Figure 22 depicts the histograms of the original information signal, an encrypted signal, and a recovered signal.

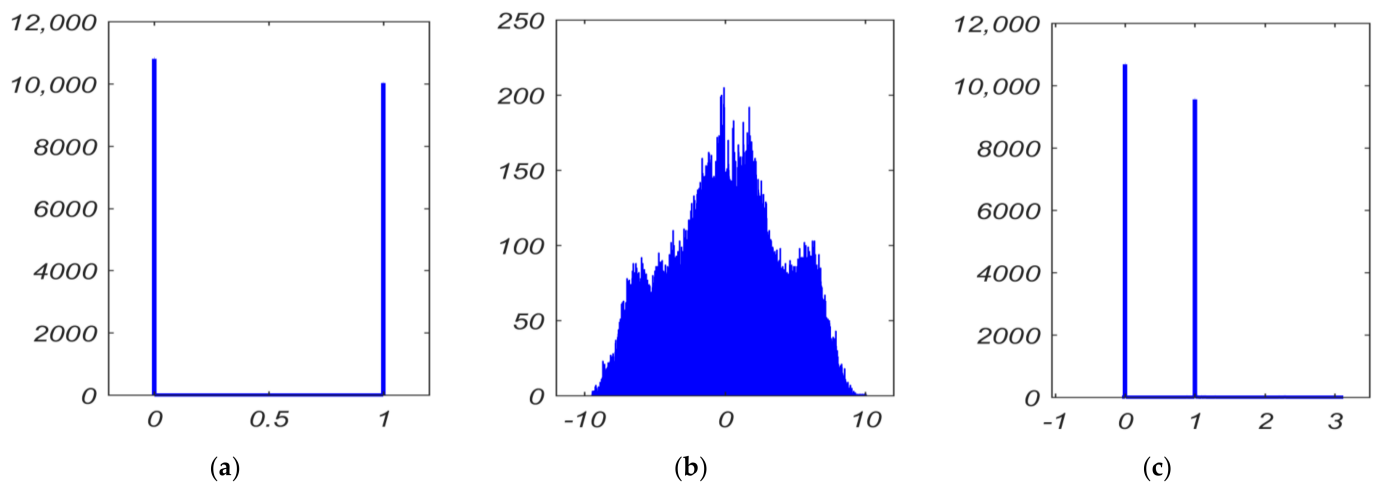


Figure 22. Histogram analysis: (a) the original information; (b) the encrypted signal; (c) the recovered signal.

When comparing the histograms in Figure 22a,b, it is clear that the distribution of the encrypted signal histograms differs significantly from that of the original signal, demonstrating the applied communication system’s high robustness against statistical or attacks. In addition, the histogram distribution for the encrypted image in Figure 22c is similar to that of the original image in Figure 22a. Thus, the original image can be successfully recovered.

9.2. Spectrogram Analysis

A spectrogram is another powerful technique for estimating the spectrum of time signals that is used in many applications [87]. A spectrogram is a plot that shows the frequency of the signal on the vertical axis, time on the horizontal axis, and signal power on a color scale to provide information about power as a function of frequency and time [88,89]. Figure 23 shows spectrograms of the original, encrypted, and recovered signals. Where the short-time Fourier transform (STFT) is used to compute the spectrogram.

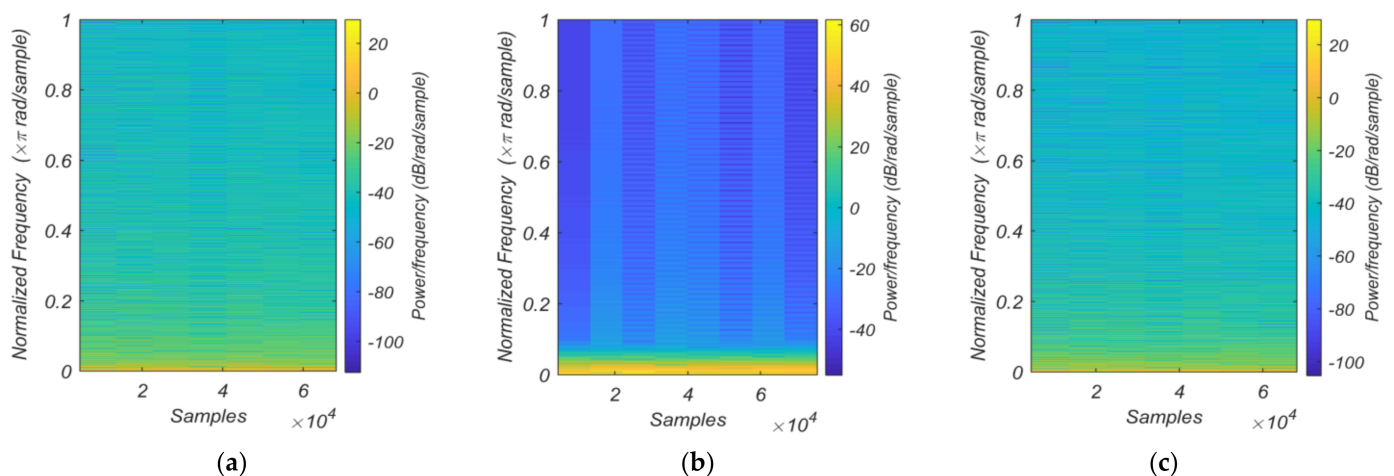


Figure 23. The spectrograms: (a) the original information; (b) the encrypted signal; (c) the recovered signal.

Figure 23 demonstrates that the original information signals differ significantly from the encrypted signals. The recovered signal, on the other hand, is similar to the original signal. As a result of these findings, high resistance against pirate attacks is provided by the employed communication system. In addition, the original image can be successfully restored.

10. Conclusions

A new FOCS is presented in this work. The dynamics of the FOCS, including the chaotic attractors, the fractal dimension, bifurcation diagrams, and Lyapunov exponent, were investigated, proving that the system exhibits very complex dynamic behaviors. Then, an adaptive synchronization technique was proposed. This technique was verified between two identical FOCSs (master and slave). Moreover, and in order to confirm the feasibility of using this new system in real applications, an analog electronic chaotic circuit was realized and examined for the proposed FOCS and its synchronization. Additionally, a microcontroller (Arduino Due) was used to demonstrate the feasibility of implementing the suggested system and the developed synchronization mechanism in real-world applications. Furthermore, the developed synchronization mechanism was used for constructing a secure communication system. Finally, the security analysis metric tests were analyzed using histograms and spectrograms to establish the communication system's security strength. The simulation results revealed that the suggested FOCS system's dynamic behavior is extremely sensitive to initial conditions, system parameters, and fractional-order derivative values (q). The simulation results obtained from MATLAB are consistent with the experimental results (analog and digital), indicating that the system is capable of being employed in real-world applications. The main advantages of using Arduino Due board to implement this system and the developed synchronization mechanism are the simplicity and low cost of implementation compared to other devices, such as FPGAs and DSPs, which are more expensive. According to the obtained results of this investigation, the proposed FOCS is simple to be implemented. Additionally, the new FOCS is very suitable to be used in high-security communication systems as it provides nonlinear dynamical behaviors with extreme complexity. The secure communication scheme is also extremely resistant to pirate attacks.

Author Contributions: Conceptualization, Z.-A.S.A.R. and B.H.J.; methodology, Z.-A.S.A.R.; software, Z.-A.S.A.R. and B.H.J.; validation, Z.-A.S.A.R. and B.H.J.; formal analysis, Z.-A.S.A.R., B.H.J. and Y.I.A.A.-Y.; investigation, Z.-A.S.A.R. and Y.-F.H.; resources, Z.-A.S.A.R., B.H.J., Y.I.A.A.-Y., R.A.A.-A. and B.N.A.; data curation, Z.-A.S.A.R. and B.H.J.; writing—original draft preparation, Z.-A.S.A.R. and B.H.J.; writing—review and editing, Z.-A.S.A.R., Y.-F.H., Y.I.A.A.-Y. and B.N.A.; visualization, Z.-A.S.A.R., B.H.J., Y.I.A.A.-Y. and B.N.A.; supervision, B.H.J. and R.A.A.-A. All authors have read and agreed to the published version of the manuscript.

Funding: This research received no external funding.

Informed Consent Statement: Not applicable.

Data Availability Statement: Not applicable.

Conflicts of Interest: The authors declare no conflict of interest.

References

1. Cao, Y. Chaotic synchronization based on fractional order calculus financial system. *Chaos Solitons Fractals* **2020**, *130*, 109410. [[CrossRef](#)]
2. Ewees, A.A.; Elaziz, M.A. Performance analysis of chaotic multi-verse harris hawks optimization: A case study on solving engineering problems. *Eng. Appl. Artif. Intell.* **2020**, *88*, 103370. [[CrossRef](#)]
3. Zhang, Z.; Kundu, S.; Tripathi, J.P.; Bugalia, S. Stability and Hopf bifurcation analysis of an SVEIR epidemic model with vaccination and multiple time delays. *Chaos Solitons Fractals* **2020**, *131*, 109483. [[CrossRef](#)]
4. Chen, H.-C.; Liau, B.-Y.; Hou, Y.-Y. Hardware implementation of Lorenz circuit systems for secure chaotic communication applications. *Sensors* **2013**, *13*, 2494–2505. [[CrossRef](#)] [[PubMed](#)]
5. Al-Hussein, A.-B.A.; Tahir, F.R.; Boubaker, O. Chaos Elimination in Power System Using Synergetic Control Theory. In Proceedings of the 2021 18th International Multi-Conference on Systems, Signals & Devices (SSD), Monastir, Tunisia, 22–25 March 2021; pp. 340–345.
6. Solano, J.; Balibrea, F.; Moreno, J.A. Applications of the Network Simulation Method to Differential Equations with Singularities and Chaotic Behaviour. *Mathematics* **2021**, *9*, 1442. [[CrossRef](#)]
7. Walleczek, J. *Self-Organized Biological Dynamics and Nonlinear Control: Toward Understanding Complexity, Chaos and Emergent Function in Living Systems*; Cambridge University Press: Cambridge, UK, 2006.

8. Babajans, R.; Cirjulina, D.; Grizans, J.; Aboltins, A.; Pikulins, D.; Zeltins, M.; Litvinenko, A. Impact of the Chaotic Synchronization's Stability on the Performance of QCPK Communication System. *Electronics* **2021**, *10*, 640. [[CrossRef](#)]
9. Zhu, X.; Chen, K.; Wang, Y.; Zheng, H. Adaptive PID controller for cloud smart city system stability control based on chaotic neural network. *Clust. Comput.* **2019**, *22*, 13067–13075. [[CrossRef](#)]
10. Eisencraft, M.; Attux, R.; Suyama, R. *Chaotic Signals in Digital Communications*; CRC Press: Boca Raton, FL, USA, 2018.
11. Tlelo-Cuautle, E.; Díaz-Muñoz, J.D.; González-Zapata, A.M.; Li, R.; León-Salas, W.D.; Fernández, F.V.; Guillén-Fernández, O.; Cruz-Vega, I. Chaotic image encryption using hopfield and hindmarsh-rose neurons implemented on FPGA. *Sensors* **2020**, *20*, 1326. [[CrossRef](#)]
12. Curiac, D.-I.; Baniias, O.; Volosencu, C.; Curiac, C.-D. Novel bioinspired approach based on chaotic dynamics for robot patrolling missions with adversaries. *Entropy* **2018**, *20*, 378. [[CrossRef](#)]
13. Zeng, Y.; Singh, S.N. Adaptive control of chaos in Lorenz system. *Dyn. Control.* **1997**, *7*, 143–154. [[CrossRef](#)]
14. Javan, A.A.K.; Shoeibi, A.; Zare, A.; Izadi, N.H.; Jafari, M.; Alizadehsani, R.; Moridian, P.; Mosavi, A.; Acharya, U.R.; Nahavandi, S. Design of Adaptive-Robust Controller for Multi-State Synchronization of Chaotic Systems with Unknown and Time-Varying Delays and Its Application in Secure Communication. *Sensors* **2021**, *21*, 254. [[CrossRef](#)] [[PubMed](#)]
15. Yuan, J.; Shi, B.; Zeng, X.; Ji, W.; Pan, T. Sliding mode control of the fractional-order unified chaotic system. *Abstr. Appl. Anal.* **2013**, *2013*, 397504. [[CrossRef](#)]
16. Daftardar-Gejji, V.; Bhalekar, S. Chaos in fractional ordered Liu system. *Comput. Math. Appl.* **2010**, *59*, 1117–1127. [[CrossRef](#)]
17. Zhang, F.; Chen, G.; Li, C.; Kurths, J. Chaos synchronization in fractional differential systems. *Philos. Trans. R. Soc. A Math. Phys. Eng. Sci.* **2013**, *371*, 20120155. [[CrossRef](#)] [[PubMed](#)]
18. Grigorenko, I.; Grigorenko, E. Chaotic dynamics of the fractional Lorenz system. *Phys. Rev. Lett.* **2003**, *91*, 34101. [[CrossRef](#)] [[PubMed](#)]
19. Peng, Z.; Yu, W.; Wang, J.; Wang, J.; Chen, Y.; He, X.; Jiang, D. Dynamic analysis of seven-dimensional fractional-order chaotic system and its application in encrypted communication. *J. Ambient. Intell. Humaniz. Comput.* **2020**, *11*, 5399–5417. [[CrossRef](#)]
20. Agarwal, P.; Chand, M.; Baleanu, D.; O'Regan, D.; Jain, S. On the solutions of certain fractional kinetic Equations involving k-Mittag-Leffler function. *Adv. Differ. Equ.* **2018**, *2018*, 249. [[CrossRef](#)]
21. Sun, H.; Zhang, Y.; Baleanu, D.; Chen, W.; Chen, Y. A new collection of real world applications of fractional calculus in science and engineering. *Commun. Nonlinear Sci. Numer. Simul.* **2018**, *64*, 213–231. [[CrossRef](#)]
22. Pham, V.-T.; Kingni, S.T.; Volos, C.; Jafari, S.; Kapitaniak, T. A simple three-dimensional fractional-order chaotic system without equilibrium: Dynamics, circuitry implementation, chaos control and synchronization. *AEU-Int. J. Electron. Commun.* **2017**, *78*, 220–227. [[CrossRef](#)]
23. Seifert, R.; Hofmann, W. Highly Dynamic Thrust Bearing Control Based on a Fractional-Order Flux Estimator. *IEEE Trans. Ind. Appl.* **2021**, *57*, 1–11. [[CrossRef](#)]
24. Boubaker, O.; Jafari, S. *Recent Advances in Chaotic Systems and Synchronization: From Theory to Real World Applications*; Elsevier: Amsterdam, The Netherlands, 2018. [[CrossRef](#)]
25. Ray, S.S.; Atangana, A.; Noutchie, S.C.; Kurulay, M.; Bildik, N.; Kilicman, A. *Fractional Calculus and Its Applications in Applied Mathematics and Other Sciences*; Hindawi: London, UK, 2014.
26. Tarasov, V.E. Mathematical Economics: Application of Fractional Calculus. *Mathematics* **2020**, *8*, 660. [[CrossRef](#)]
27. Rahman, Z.-A.S.A.; Jasim, B.H.; Al-Yasir, Y.I.A.; Abd-Alhameed, R.A.; Alhasnawi, B.N. A New No Equilibrium Fractional Order Chaotic System, Dynamical Investigation, Synchronization, and Its Digital Implementation. *Inventions* **2021**, *6*, 49. [[CrossRef](#)]
28. Mobini, M.; Kaddoum, G. Deep chaos synchronization. *IEEE Open J. Commun. Soc.* **2020**, *1*, 1571–1582. [[CrossRef](#)]
29. Karthikeyan, A.; Rajagopal, K. FPGA implementation of fractional-order discrete memristor chaotic system and its commensurate and incommensurate synchronisations. *Pramana* **2018**, *90*, 14. [[CrossRef](#)]
30. Hu, J.; Liu, B.; Yu, M. A Novel Method of Realizing Stochastic Chaotic Secure Communication by Synchrosqueezed Wavelet Transform: The Finite-time Case. *IEEE Access* **2021**, *9*, 1. [[CrossRef](#)]
31. He, S.; Sun, K.; Wang, H.; Mei, X.; Sun, Y. Generalized synchronization of fractional-order hyperchaotic systems and its DSP implementation. *Nonlinear Dyn.* **2018**, *92*, 85–96. [[CrossRef](#)]
32. Rahman, Z.-A.S.A.; Al-Kashoash, H.A.A.; Ramadhan, S.M.; Al-Yasir, Y.I.A. Adaptive Control Synchronization of a Novel Memristive Chaotic System for Secure Communication Applications. *Inventions* **2019**, *4*, 30. [[CrossRef](#)]
33. Lin, C.-M.; Pham, D.-H.; Huynh, T.-T. Synchronization of Chaotic System Using a Brain-Imitated Neural Network Controller and Its Applications for Secure Communications. *IEEE Access* **2021**, *9*, 75923–75944. [[CrossRef](#)]
34. Velamore, A.A.; Hegde, A.; Khan, A.A.; Deb, S. Dual cascaded Fractional-order Chaotic Synchronization for Secure Communication with Analog Circuit Realisation. In Proceedings of the 2021 IEEE Second International Conference on Control, Measurement and Instrumentation (CMI), Kolkata, India, 8–10 January 2021; pp. 30–35.
35. Jasim, B.H.; Hassan, K.H.; Omran, K.M. A new 4-D hyperchaotic hidden attractor system: Its dynamics, coexisting attractors, synchronization and microcontroller implementation. *Int J. Electr. Comput. Eng.* **2021**, *11*, 2068–2078.
36. Jasim, B.H.; Mjily, A.H.; AL-Aaragee, A.M.J. A novel 4 dimensional hyperchaotic system with its control, synchronization and implementation. *Int. J. Electr. Comput. Eng.* **2021**, *11*, 2974–2985.
37. Fujisaka, H.; Yamada, T. Stability theory of synchronized motion in coupled-oscillator systems. *Prog. Theor. Phys.* **1983**, *69*, 32–47. [[CrossRef](#)]

38. Da-Wei, D.; Fang-Fang, L.; Hui, C.; Nian, W.; Dong, L. Sliding Mode Control of Fractional-Order Delayed Memristive Chaotic System with Uncertainty and Disturbance. *Commun. Theor. Phys.* **2017**, *68*, 741.
39. Hou, J.; Xi, R.; Liu, P.; Liu, T. The switching fractional order chaotic system and its application to image encryption. *IEEE/CAA J. Autom. Sin.* **2016**, *4*, 381–388. [[CrossRef](#)]
40. Dutta, M.; Roy, B.K. A new fractional-order system displaying coexisting multiwing attractors; its synchronisation and circuit simulation. *Chaos Solitons Fractals* **2020**, *130*, 109414. [[CrossRef](#)]
41. Rashidnejad, Z.; Karimaghaee, P. Synchronization of a class of uncertain chaotic systems utilizing a new finite-time fractional adaptive sliding mode control. *Chaos, Solitons Fractals X* **2020**, *5*, 100042. [[CrossRef](#)]
42. Ahmad, M.; Shamsi, U.; Khan, I.R. An enhanced image encryption algorithm using fractional chaotic systems. *Procedia Comput. Sci.* **2015**, *57*, 852–859. [[CrossRef](#)]
43. Martínez-Guerra, R.; Gómez-Cortés, G.C.; Pérez-Pinacho, C.A. Synchronization of integral and fractional order chaotic systems. In *A Differential Algebraic and Differential Geometric Approach with Selected Applications in Real-Time*; Springer: Berlin/Heidelberg, Germany, 2015.
44. Martínez-Guerra, R.; Pérez-Pinacho, C.A. *Advances in Synchronization of Coupled Fractional Order Systems: Fundamentals and Methods*; Springer: Berlin/Heidelberg, Germany, 2018.
45. Kharel, R. Design and Implementation of Secure Chaotic Communication Systems. Ph.D. Thesis, Northumbria University, Newcastle upon Tyne, UK, 2011.
46. Gonzalez, E.A.; Petráš, I. Advances in fractional calculus: Control and signal processing applications. In Proceedings of the 2015 16th International Carpathian Control Conference (ICCC), Szilvasvarad, Hungary, 27–30 May 2015; pp. 147–152.
47. Caputo, M.; Fabrizio, M. A new definition of fractional derivative without singular kernel. *Progr. Fract. Differ. Appl.* **2015**, *1*, 1–13.
48. Sene, N. Analysis of a fractional-order chaotic system in the context of the Caputo fractional derivative via bifurcation and Lyapunov exponents. *J. King Saud Univ.* **2021**, *33*, 101275. [[CrossRef](#)]
49. Li, H.-L.; Zhang, L.; Hu, C.; Jiang, Y.-L.; Teng, Z. Dynamical analysis of a fractional-order predator-prey model incorporating a prey refuge. *J. Appl. Math. Comput.* **2017**, *54*, 435–449. [[CrossRef](#)]
50. Godinho, C.F.D.L.; Panza, N.; Weberszpil, J.; Helayël-Neto, J.A. Variational procedure for higher-derivative mechanical models in a fractional integral. *EPL (Europhysics Lett.)* **2020**, *129*, 60001. [[CrossRef](#)]
51. Li, H.-L.; Jiang, H.; Cao, J. Global synchronization of fractional-order quaternion-valued neural networks with leakage and discrete delays. *Neurocomputing* **2020**, *385*, 211–219. [[CrossRef](#)]
52. Jalalinejad, H.; Tavakoli, A.; Zarmehi, F. A simple and flexible modification of Grünwald–Letnikov fractional derivative in image processing. *Math. Sci.* **2018**, *12*, 205–210. [[CrossRef](#)]
53. Atangana, A.; Gómez-Aguilar, J.F. Numerical approximation of Riemann–Liouville definition of fractional derivative: From Riemann–Liouville to Atangana–Baleanu. *Numer. Methods Partial Differ. Equ.* **2018**, *34*, 1502–1523. [[CrossRef](#)]
54. Ma, C.; Mou, J.; Liu, J.; Yang, F.; Yan, H.; Zhao, X. Coexistence of multiple attractors for an incommensurate fractional-order chaotic system. *Eur. Phys. J. Plus* **2020**, *135*, 95. [[CrossRef](#)]
55. Liu, T.; Yan, H.; Banerjee, S.; Mou, J. A fractional-order chaotic system with hidden attractor and self-excited attractor and its DSP implementation. *Chaos Solitons Fractals* **2021**, *145*, 110791. [[CrossRef](#)]
56. Gong, L.; Wu, R.; Zhou, N. A New 4D Chaotic system with coexisting hidden chaotic attractors. *Int. J. Bifurc. Chaos* **2020**, *30*, 2050142. [[CrossRef](#)]
57. Zhou, C.; Yang, C.; Xu, D.; Chen, C. Dynamic analysis and synchronisation control of a novel chaotic system with coexisting attractors. *Pramana* **2020**, *94*, 19. [[CrossRef](#)]
58. Lai, Q.; Wan, Z.; Kuate, P.D.K.; Fotsin, H. Coexisting attractors, circuit implementation and synchronization control of a new chaotic system evolved from the simplest memristor chaotic circuit. *Commun. Nonlinear Sci. Numer. Simul.* **2020**, *89*, 105341. [[CrossRef](#)]
59. Garrappa, R. Numerical Solution of Fractional Differential Equations: A Survey and a Software Tutorial. *Mathematics* **2018**, *6*, 16. [[CrossRef](#)]
60. Wu, J.; Wang, G.; Iu, H.H.-C.; Shen, Y.; Zhou, W. A nonvolatile fractional order memristor model and its complex dynamics. *Entropy* **2019**, *21*, 955. [[CrossRef](#)]
61. Dellnitz, M.; Field, M.; Golubitsky, M.; Hohmann, A.; Ma, J. Cycling chaos. *IEEE Trans. Circuits Syst. I Fundam Theory Appl.* **1995**, *42*, 821–823. [[CrossRef](#)]
62. Eshaghi, S.; Ghaziani, R.K.; Ansari, A. Hopf bifurcation, chaos control and synchronization of a chaotic fractional-order system with chaos entanglement function. *Math. Comput. Simul.* **2020**, *172*, 321–340. [[CrossRef](#)]
63. Li, T.; Wang, Y.; Zhou, X. Bifurcation analysis of a first time-delay chaotic system. *Adv. Differ. Equ.* **2019**, *2019*, 78. [[CrossRef](#)]
64. Tlelo-Cuautle, E.; Pano-Azucena, A.D.; Guillén-Fernández, O.; Silva-Juárez, A. *Analog/Digital Implementation of Fractional Order Chaotic Circuits and Applications*; Springer: Berlin/Heidelberg, Germany, 2020.
65. Collantoni, E.; Madan, C.R.; Meneguzzo, P.; Chiappini, I.; Tenconi, E.; Manara, R.; Favaro, A. Cortical complexity in anorexia nervosa: A fractal dimension analysis. *J. Clin. Med.* **2020**, *9*, 833. [[CrossRef](#)]
66. Mayor, D.; Panday, D.; Kandel, H.K.; Steffert, T.; Banks, D. CEPS: An Open Access MATLAB Graphical User Interface (GUI) for the Analysis of Complexity and Entropy in Physiological Signals. *Entropy* **2021**, *23*, 321. [[CrossRef](#)]

67. Shamsi, E.; Ahmadi-Pajouh, M.A.; Ala, T.S. Higuchi fractal dimension: An efficient approach to detection of brain entrainment to theta binaural beats. *Biomed. Signal. Process Control* **2021**, *68*, 102580. [[CrossRef](#)]
68. Kesić, S.; Spasić, S.Z. Application of Higuchi's fractal dimension from basic to clinical neurophysiology: A review. *Comput. Methods Programs Biomed.* **2016**, *133*, 55–70. [[CrossRef](#)]
69. Gatfaoui, H.; De Peretti, P. Testing for non-chaoticity under noisy dynamics using the largest Lyapunov exponent. *Soft Comput.* **2019**, *24*, 8617–8626. [[CrossRef](#)]
70. Jasim, B.H.; Rashid, M.T.; Omran, K.M. Synchronization and tracking control of a novel 3 dimensional chaotic system. *Iraqi J. Electr. Electron. Eng. Basrah University. 3RD.* **2020**, *1*, 1–6.
71. Rahman, Z.-A.S.A.; Jassim, B.H.; Al-Yasir, Y.I.A. New Fractional Order Chaotic System: Analysis, Synchronization, and it's Application. *Iraqi J. Electr. Electron. Eng.* **2021**, *17*, 1–9. [[CrossRef](#)]
72. Kaddoum, G. Wireless chaos-based communication systems: A comprehensive survey. *IEEE Access* **2016**, *4*, 2621–2648. [[CrossRef](#)]
73. Tahir, F.R.; Jafari, S.; Pham, V.-T.; Volos, C.; Wang, X. A novel no-equilibrium chaotic system with multiwing butterfly attractors. *Int. J. Bifurc. Chaos* **2015**, *25*, 1550056. [[CrossRef](#)]
74. Tahir, S.A. The synchronization of identical Memristors systems via Lyapunov direct method. *Appl. Comput. Math.* **2013**, *6*, 130–136. [[CrossRef](#)]
75. Guo, R. A simple adaptive controller for chaos and hyperchaos synchronization. *Phys. Lett. A* **2008**, *372*, 5593–5597. [[CrossRef](#)]
76. Peng, R.; Jiang, C.; Guo, R. Stabilization of a class of fractional order systems with both uncertainty and disturbance. *IEEE Access* **2021**, *9*, 42697–42706. [[CrossRef](#)]
77. Fan, X.; Wang, Z. A Fuzzy Lyapunov Function Method to Stability Analysis of Fractional Order T-S Fuzzy Systems. *IEEE Trans. Fuzzy Syst.* **2021**, *29*, 1–9.
78. Ahmad, W.M.; Sprott, J.C. Chaos in fractional-order autonomous nonlinear systems. *Chaos Solitons Fractals* **2003**, *16*, 339–351. [[CrossRef](#)]
79. Pu, Y.-F. Measurement units and physical dimensions of fractance-part I: Position of purely ideal fractor in Chua's axiomatic circuit element system and fractional-order reactance of fractor in its natural implementation. *IEEE Access* **2016**, *4*, 3379–3397. [[CrossRef](#)]
80. Hammouch, Z.; Mekkaoui, T. Circuit design and simulation for the fractional-order chaotic behavior in a new dynamical system. *Complex Intell. Syst.* **2018**, *4*, 251–260. [[CrossRef](#)]
81. Sánchez-López, C. An experimental synthesis methodology of fractional-order chaotic attractors. *Nonlinear Dyn.* **2020**, *100*, 3907–3923. [[CrossRef](#)]
82. Due, A. Core ARM. Arduino Due. Retrieved **2017**, *9*, 2019.
83. Çiçek, S.; Ferikoğlu, A.; Pehlivan, İ. A new 3D chaotic system: Dynamical analysis, electronic circuit design, active control synchronization and chaotic masking communication application. *Optik* **2016**, *127*, 4024–4030. [[CrossRef](#)]
84. Hashemi, S.; Pourmina, M.A.; Mobayen, S.; Alagheband, M.R. Design of a secure communication system between base transmitter station and mobile equipment based on finite-time chaos synchronisation. *Int. J. Syst. Sci.* **2020**, *51*, 1969–1986. [[CrossRef](#)]
85. Alanazi, A.S.; Munir, N.; Khan, M.; Asif, M.; Hussain, I. Cryptanalysis of Novel Image Encryption Scheme Based on Multiple Chaotic Substitution Boxes. *IEEE Access* **2021**, *9*, 93795–93802. [[CrossRef](#)]
86. Yasser, I.; Mohamed, M.A.; Samra, A.S.; Khalifa, F. A chaotic-based encryption/decryption framework for secure multimedia communications. *Entropy* **2020**, *22*, 1253. [[CrossRef](#)] [[PubMed](#)]
87. Kacha, A.; Grenez, F.; Orozco-Arroyave, J.R.; Schoentgen, J. Principal component analysis of the spectrogram of the speech signal: Interpretation and application to dysarthric speech. *Comput. Speech Lang.* **2020**, *59*, 114–122. [[CrossRef](#)]
88. Bruni, V.; Tartaglione, M.; Vitulano, D. A pde-Based Analysis of the Spectrogram Image for Instantaneous Frequency Estimation. *Mathematics* **2021**, *9*, 247. [[CrossRef](#)]
89. Karimov, T.; Rybin, V.; Kolev, G.; Rodionova, E.; Butusov, D. Chaotic Communication System with Symmetry-Based Modulation. *Appl. Sci.* **2021**, *11*, 3698. [[CrossRef](#)]